UNIVERSIDADE DA BEIRA INTERIOR
Ciências da Saúde

Are polyamines detected by the TAAR receptor family in the human Choroid Plexus?

Duarte Nuno de Almeida Santos e Lopes Rocha

Dissertação para obtenção do Grau de Mestre em
Ciências Biomédicas
(2º ciclo de estudos)

Orientador: Profª. Doutora Cecília Reis Alves Santos
Co-orientador: Profª. Doutora Isabel Maria Theriaga M. V. Gonçalves

Covilhã, junho de 2018

Acknowledgments

There are diverse people without them this work wouldn´t had been possible, so I must thank them.

To my supervisor, PhD Professor Cecília Santos for accepting me in her research group, for enabling me to work on a subject I like, for all scientific knowledge and for the guidance and help during this year.

To my co-supervisor, PhD Professor Isabel Gonçalves for the support in laboratory activities, for all the scientific knowledge transmitted and for the guidance, help and availability during this year.

To Dr Helena Marcelino, Joana Tomás and Dr Telma Quintela for their support in laboratory activities, their advices, suggestions and availability.

To PhD students Catarina Duarte, Ana Costa, Ana Brito and Daniela Talhada for all their support during this year, for the way they received me and helped me to take the first steps in the laboratory work, for all the advices, support and friendship.

To my group colleague and friend José Santos, for his friendship, availability, for his help with laboratory work and when I had to face less good situations.

To my colleagues Bruno Baptista, Rúben Faria and Rui Carrilho for their friendship and for being always available to help me with my work.

To my mother Alexandra Almeida Santos, and my brother Afonso Rocha for their support and comprehension during this year, without them this work would not have been possible.

To my grandparents Albino e Maria Néli Almeida Santos that although they are no longer among us, they would certainly be very proud to see me complete this phase of my academic life.

To my remaining family and friends for all their support, comprehension and friendship.

This work was partially supported by ‘‘Programa Operacional do Centro, Centro 2020” through the funding of the ICON project (Interdisciplinary Challenges On Neurodegeneration; CENTRO-01-0145-FEDER-000013)”.

Abstract

Choroid plexuses (CPs) are highly vascularized structures located at the ventricular system of the brain constituted by a monolayer of choroid plexus epithelial cells (CPEC) located on a basement membrane which form a barrier between the blood and the cerebrospinal fluid (CSF) (BCSFB). CPECs through their interconnections restrict the passage of different substances and pathogens between the blood and the CSF. Moreover, the microvilli at the apical side and an extensive infolding at the basolateral side enhance the contact between the CP epithelium and CSF, and between the epithelium and stroma interstitial fluid, respectively, thus allowing one of its main functions which is to maintain cerebral homeostasis. Among other features, there is the chemical vigilance which is performed by different mechanisms as the taste signalling, the clearance of xenobiotics, the clearance of amyloid beta and finally but with more relevance to this work, the olfactory signalling.

This olfactory cascade is activated when an odorant binds to an olfactory receptor (OR) which is a G protein-coupled receptor (GPCR) that exists in different tissues in mammalian´s body. The trace amine-associated receptors (TAARs) are a family of rhodopsin-like GPCRs which act as olfactory receptors with TAAR1 exception and are expressed in different tissues of different species. In humans there are 6 different types of TAARs and 3 pseudogenes. TAAR 13c, identified in zebrafish, can bind to cadaverine, a polyamine. Polyamines are polycations which appear naturally in cells and are closely related with neuronal cell biochemical activity at different points. Cadaverine is a diamine compound produced by the putrefaction of animal tissue and enable an aversive response to this odour. A previous data base research showed that TAAR1, 2 and 5 are the human receptors with more homology with TAAR13c and one of the more abundant TAARs in humans, which probably can trigger a response to a polyamine stimulus. TAAR1 was selected for this study because we could not amplify TAAR2 and 5 by RT-PCR in HIBCPP cell line.

The HIBCPP cell line from choroid plexus carcinoma was used to the experiments and the expression of the mRNAs to the TAAR1 was demonstrated by the RT-PCR technique. In respect to polyamine´s biosynthesis and catabolic pathway enzymes identification, the RT-PCR technique enabled the confirmation of their mRNA expression after Sanger sequencing. The expression of key enzymes to these pathways was also demonstrated by immunocytochemistry and Western blot, in human CP cell line.

To test the cell´s response to polyamines, calcium imaging (Ca^{2+} imaging) assays were performed and showed clear responses to cadaverine. After these tests, silencing of TAAR1 with a specific small interfering RNA (siRNA) was done and preliminary Ca^{2+} imaging responses

to cadaverine enable to see a decrease in CP cells response, highlighting the potential role of TAAR1 in this polyamine response.

In the closer future, more silencing assays will be done and Ca^{2+} imaging with transfected cells will be done too with cadaverine and other polyamines already tested as spermine, spermidine and putrescine. Western blot and immunocytochemistry techniques will enable the TAAR1 protein characterization and localization in the HIBCPP cells.

Keywords

Brain barriers, choroid plexus, olfactory receptor, polyamines, trace amine associated receptors.

Resumo alargado

No sistema nervoso central (SNC) é possível observar a presença de distintas barreiras que assumem um papel fundamental na proteção do cérebro contra as variações nas concentrações de determinadas substâncias ao nível do sangue, assim como contra a entrada de organismos patogénicos, toxinas e outras substâncias. Contudo, este nem sempre é um mecanismo de controlo favorável uma vez que estas podem funcionar como uma barreira à entrada de substâncias para o tratamento de patologias do SNC. De entre as barreiras existentes no cérebro salienta-se a barreira entre o sangue e o cérebro, a barreira aracnóideia e a barreira entre o sangue e o líquido cefalorraquidiano, o plexo coroide.

O plexo coroide (CP) é uma estrutura altamente vascularizada localizada em cada um dos quatro ventrículos cerebrais. O CP é constituído por uma monocamada de células epiteliais localizada numa membrana basal e que por sua vez, formam uma barreira entre o sangue e o líquido cefalorraquidiano. Estas células, através das suas interconexões como é o caso das junções aderentes, junções apertadas e desmossomas, impedem a passagem de diferentes substâncias e organismos patogénicos, do sangue para o líquido cefalorraquidiano. Para além destas evidências, há a destacar o facto de as microvilosidades presentes na face apical assim como as invaginações existentes na superfície basal permitirem também uma boa interação entre o epitélio do plexo e o líquido cefalorraquidiano e entre o epitélio e o fluido intersticial, respetivamente, permitindo um conjugar de condições que vão assegurar uma correta manutenção da homeostase cerebral. De entre outras funções desempenhadas por esta estrutura, salienta-se a produção e secreção do líquido cefalorraquidiano e a vigilância química deste, que é assegurada por diferentes mecanismos como a sinalização gustativa, a remoção de xenobióticos, a remoção da proteína ß-amilóide, envolvida em doenças como a doença de Alzheimer, e por fim a sinalização olfativa.

Esta cascata de sinalização olfativa é ativada quando uma molécula odorante se liga a um recetor olfativo, um recetor acoplado a uma proteína G. Esta ligação vai despoletar as cascatas de segundo mensageiro da adenosina monofosfato cíclica e do inositol 1,4,5-trifosfato. Há evidências de que a estimulação destes recetores olfativos ocorre pela ativação da proteína G olfativa levando a um aumento da adenosina monofosfato cíclica através da adenilato ciclase 3 de membrana, resultando num aumento do influxo de Ca^{2+} através de um canal nucleotídico cíclico, resultando na despolarização da membrana e consequentemente na geração de um potencial de ação nos neurónios olfativos.

Os *trace amine-associated receptors* (TAARs) são uma família de recetores acoplados a proteína G que, à exceção do TAAR1, atuam como recetores olfativos, sendo expressos em diferentes tecidos em diferentes espécies. Diferentes estudos permitiram comprovar a

expressão destes recetores em tecidos do epitélio olfativo e noutros como é o caso do cérebro, medula espinhal, coração, pulmões, fígado, baço, trato gastrointestinal, rins, testículos e células sanguíneas como os leucócitos. Em humanos é possível identificar 6 tipos diferentes de TAARs (1,2,5,6,8 e 9) e 3 pseudogenes (3, 4 e 7). Os genes que codificam para estes recetores encontram-se localizados no cromossoma 6 q23.1. O TAAR13c, expresso no peixe-zebra foi identificado como sendo o responsável por ligar à cadaverina, uma poliamina resultante da decomposição de tecidos mortos, gerada através da descarboxilação da lisina pela enzima lisina-descarboxílase, que ao ser detetada por este peixe, despoleta uma resposta aversiva por parte deste.

As poliaminas são policatiões presentes em todas as células, que interagem com moléculas carregadas negativamente como é o caso do ácido desoxirribonucleico (DNA), ácido ribonucleico (RNA) ou ainda as proteínas. Estas substâncias como é o caso da cadaverina, espermina, espermidina e putrescina participam em diversas funções a nível fisiológico como o crescimento celular, proliferação, diferenciação, transcrição, tradução, regulação de canais iónicos, atividade enzimática, constituição das interações célula-célula e resposta ao stress oxidativo. Estas duas últimas funções conferem às poliaminas um papel fundamental no surgimento de diversas patologias do foro neurológico como é o caso da doença Parkinson, da esclerose lateral amiotrófica e isquemia, em que os valores destas substâncias surgem alterados. Contudo as poliaminas ao controlarem o stress oxidativo vão também ter um papel benéfico no controlo da doença de Alzheimer.

Com o objetivo de estabelecer homologia entre o TAAR13c *do* peixe-zebra e os TAARs humanos foi realizada uma pesquisa com a ferramenta BlastX (NCBI) que revelou a existência de diferentes TAAR com maior homologia com o TAAR13c. Após uma pesquisa na base de dados *Gene Expression Omnibus*, foram selecionados para o estudo, os TAAR1, 2 e 5 por estes apresentarem maior abundância em humanos. Estes dados levaram-nos a supor que estes recetores teriam capacidade para despoletar uma resposta em células humanas do plexo coroide quando estimuladas por poliaminas como a cadaverina.

Assim, o uso de uma linha de células humanas de carcinoma do plexo coroide, através da técnica de RT-PCR seguida de sequenciação pelo método de Sanger, permitiu identificar a expressão do mRNA para o TAAR1, o que não se verificou para os TAAR2 e 5. Um processo idêntico foi utilizado para a análise da expressão dos mRNAs para as enzimas das vias anabólica e catabólica das poliaminas, sendo a sua expressão confirmada por sequenciação. As enzimas chave destas vias, a espermina sintetase e a ornitina descarboxílase, foram também analisadas através das técnicas de *Western blot* e imunocitoquímica.

Após a realização de um ensaio de MTT que permitiu comprovar que os estímulos de cadaverina aplicados não iriam comprometer a viabilidade celular, foram realizados ensaios

de *calcium imaging* que possibilitaram verificar respostas por parte das células após estimulação com diferentes concentrações de cadaverina.

Por forma e testar a especificidade da ligação do TAAR1 à cadaverina, foi realizado um ensaio preliminar (n=1) de silenciamento, transfetando as células com um pequeno RNA de interferência (siRNA) para o TAAR1. Os resultados demonstraram uma diminuição das respostas celulares à cadaverina quando em comparação com os controlos feitos apenas com o agente de transfeção ou com este último em conjunto com um *scramble* siRNA. Estes resultados, embora preliminares, são promissores quanto ao papel do TAAR1 na deteção da cadaverina.

Futuramente, serão realizados novos ensaios de silenciamento do TAAR1 e estímulos com outras poliaminas como a espermina, espermidina e putrescina. Serão também efetuados ensaios de *Western blot* e imunocitoquímica, permitindo avaliar a expressão e localização do TAAR1.

Palavras-chave

Barreiras cerebrais, plexo coróide, poliaminas, recetores olfativos, *trace amine associated receptors*.

Index

Figures list

Tables list

Abbreviations and Acronymes List

AC3	Adenylate Cyclase 3
Aß	Amyloid Beta
Acetyl-CoA	Acetyl Coenzyme A
AD	Alzheimer´s Disease
AdoMet	S-adenosyl-L-methionine
AJs	Adherent Junctions
AKT	Protein Kinase B
ALS	Amyotrophic Lateral Sclerosis
APP	Amyloid Beta Precursor Protein
AQP1	Aquaporin 1
Azin1	Antienzyme 1
BBB	Blood-Brain Barrier
BCSFB	Blood-Cerebrospinal Fluid Barrier
B-PEA	ß-Phenylethylamine
BSA	Bovine Serum Albumin
Ca^{2+}	Calcium ion
cAMP	Adenosine 3´,5´-Cyclic Monophosphate
cDNA	Complementary Deoxyribonucleic Acid
Cl^-	Chlorine ion
CNG2	Cyclic Nucleotide-Gated Channel 2
CNS	Central Nervous System
CO_2	Carbon Dioxyde
CP	Choroid Plexus
CPE	Choroid Plexus Epithelium
CPEC	Choroid Plexus Epithelial Cells
CSF	Cerebrospinal Fluid
DA	Dopamine
DAG	Diacyl Glycerol
DAT	Dopamine Transporter
DcAdoMet	Decarboxylated S-adenosyl-L-methionine
DEPC	Diethylpyrocarbonate
DMEM/F12	Dulbecco's Modified Eagle Medium: Nutrient Mixture F-12
DMSO	Dimethyl Sulfoxide
DNA	Deoxyribonucleic Acid
dNTPs	Deoxyribonucleotides Triphosphate
DR	Dopamine Receptor
EC_{50}	Half Maximal Effective Concentration
EDTA	Ethylenediamine Tetraacetate
FBS	Fetal Bovine Serum
GABA	Gamma-aminobutyric Acid
GFs	Growth Factors
G_{olf}	Olfactory G Protein
GPCR	G Protein-Coupled Receptors
G Protein	Guanine Nucleotide-binding Proteins

GSK-3	Kinase B/glycogen synthase kinase 3
HIBCPP	Human Malignant Choroid Plexus Papilloma Cell Line
IP_3	Inositol 1,4,5-trisphosphate
IP_3R3	Type 3 Receptor Ion Channels
LDC	Lysine Decarboxylase
MCR	Multiple Cloning Region
mRNA	Messenger Ribonucleic Acid
MTT	3-(4,5-dimethylthiazol-2-yl)-2,5-diphenyltetrazolium bromide
Na^+	Sodium ion
Oaz1	Ornithine Decarboxylase Antienzime 1
ODC1	Ornithine Decarboxylase
OMP	Olfactory Marker Protein
ORI	Replication Origin
ORs	Olfactory Receptors
OSNs	Olfactory Sensorial Neurons
PA	Polyamine
PAs	Polyamines
PAO	Polyamine Oxidase
PBS	Phosphate Buffered Saline
PBS-T	Phosphate Buffered Saline - Tween
PCR	Polymerase Chain Reaction
PD	Parkinson´s Disease
PFA	Paraformaldehyde
PI3K	Phosphoinositide 3-kinase
PLC	Phospholipase-C
PLC-β2	Phospholipase-C beta2
PSA	Ammonium Persulfate
RNA	Ribonucleic Acid
rRNA	Ribosomal Ribonucleic Acid
RT-PCR	Reverse Transcriptase-Polymerase Chain Reaction
SAMdc (AMD1)	S-adenosylmethionine Decarboxylase
SDS	Sodium Dodecyl Sulphate
SH	Sex Hormones
siRNA	Small Interferring Ribonucleic Acid
SMO	Spermine Oxidase
SNP	Single Nucleotide Polymorphism
SPSY (Sms)	Spermine Synthase
Srm	Spermidine Synthase
SSAT	Spermidine/Spermine N´-acetyltransferase
TBS	Tris-buffered Saline
TBS-T	Tris-buffered Saline - Tween
TJs	Tight Junctions
TAAR	Trace Amine-Associated Receptor
TRs	Taste Receptors
TrpM5	Transient Receptor Potential Channel M5
VTA	Ventral Tegmental Area

Chapter 1

1. Introduction

1. Introduction

1.1 Brain Barriers

Brain barriers play a key role protecting the brain from the concentration´s variation of different molecules in the blood preventing the entrance of pathogens, toxins and many other compounds. But the control of some substance´s passage from blood to the brain is not always a beneficial mechanism since, when administering to a patient a certain dose of a drug to treat diseases as brain tumours or dementia, its bioavailability in the brain will be affected by these barrier mechanisms (Tietz & Engelhardt 2015; Marques et al. 2017). The restricted penetration of these drugs into the brain results from different mechanisms which contributes for the maintenance of brain extracellular fluid homeostasis which will be discussed later in this section (Ghersi-Egea et al. 2009).

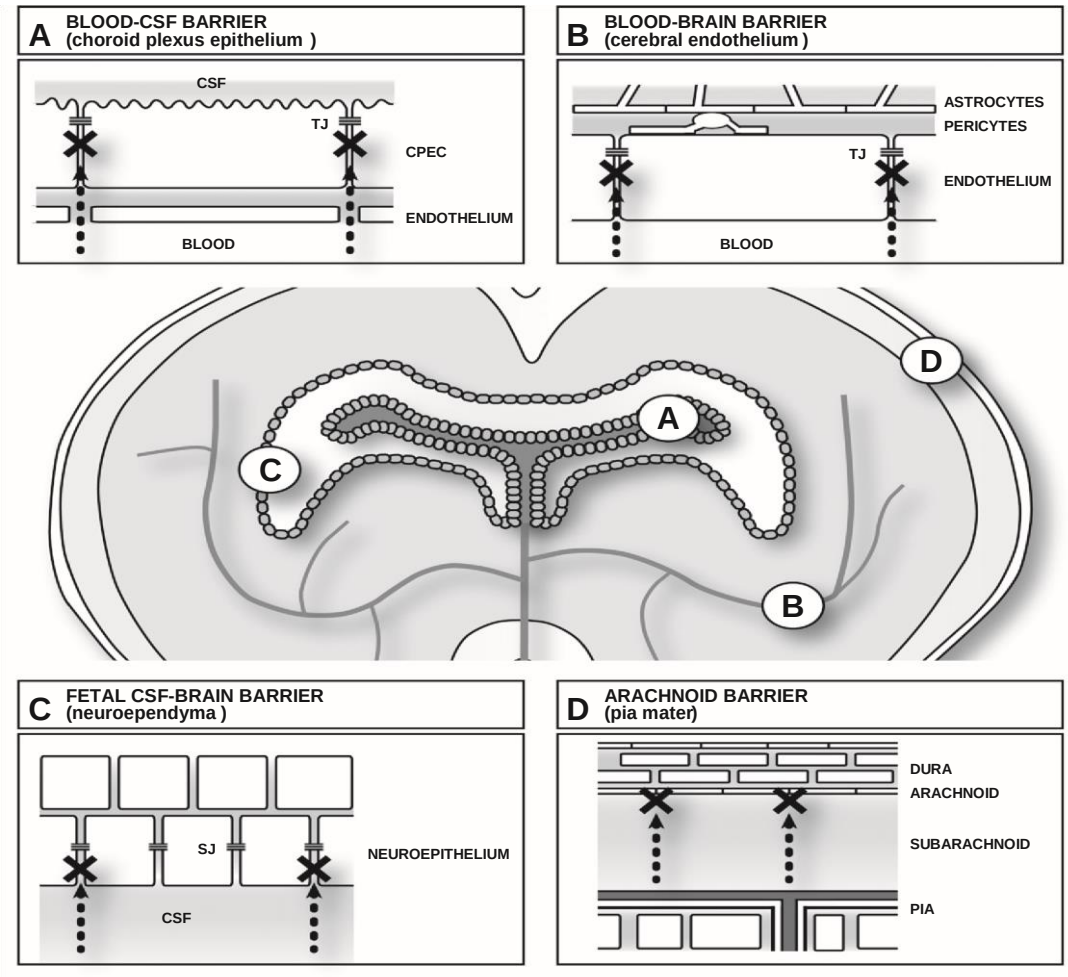

Figure 1 – **Barriers of the brain.** Adapted from (Saunders et al. 2013) **A.** BCSFB is a brain barrier between blood vessels in choroid plexus (CP) and the cerebrospinal fluid (CSF). Tight junctions (TJs) in choroid plexus epithelial cells (CPEC) restrict intracellular molecular passage; **B.** BBB separates the nervous system from the circulating blood; **C.** Fetal CSF-brain barrier is located between the CSF and the neuroependyma. Neuroependymal cells are connected by strap junctions preventing large molecules exchange between CSF and brain. This barrier is only present in early developing brain because of the loss of the strap junctions and the conversion of the neuroependyma to ependyma; **D.** Arachnoid barrier is located between the CSF-filled subarachnoid space and the overlying structures. The fenestrated blood vessels present in the *dura* provide a weak barrier function.

There are three interfaces separating the blood and the central nervous system (CNS): the blood-brain barrier (BBB), the blood-cerebrospinal fluid barrier (BCSFB) and the arachnoid barrier (Figure 1). These control the entry or exit of different molecules and pathogens reaching the brain (Abbott et al. 2010; Saunders et al. 2013).

The blood-brain barrier (BBB) is the largest and a very tight barrier in the brain, formed by endothelial cells of the capillaries. It separates the nervous system from the circulating blood (Abbott et al. 2010).

The arachnoid barrier is located underlying dura mater and encloses the CNS completing the seal between the cellular fluids of the CNS and the rest of the body. Because it is avascular nature, this barrier does not act as a surface for important exchanges between the blood and the CNS (Abbott et al. 2010).

The blood-cerebrospinal fluid barrier (BCSFB), whose apical face has a half of the area of the BBB, is the choroid plexus epithelium (CPE). The tight junctions (TJs) between the choroid plexus epithelial cells (CPEC), composed by occludin and claudins 1, 2 and 11, have a fundamental role in controlling the passage of solutes like water, ions and other small molecules, as well as cell migration to the CSF, and in facilitating the removal of toxic compounds. Although relatively large molecules can pass by the fenestrated endothelial cells and leaky capillaries in CP, the carriers and transporters present in CPEC can restrict the passage of these molecules into CSF, then contributing to homeostasis (Saunders et al. 2013; Danielski et al. 2017; Praetorius & Damkier 2017).

1.1.1 The Blood-cerebrospinal Fluid Barrier-the Choroid Plexus

The choroid plexuses are highly vascularized structures located at the ventricular system of the brain (Figure 2). They are sheet-like shaped, attached to the ependyma by a stalk and float on the cerebrospinal fluid, which fills the ventricles (Falcão et al. 2012; Damkier et al. 2013; Santos et al. 2017).

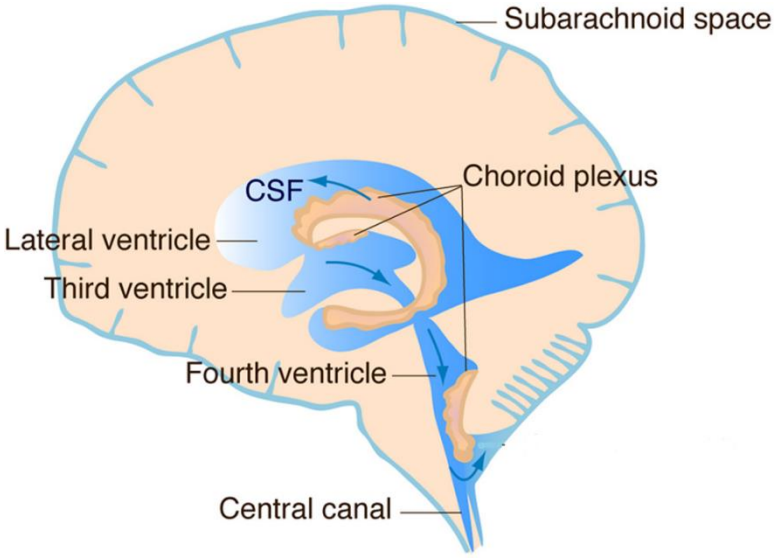

Figure 2 – **Choroid plexus (CP) localization in the ventricular system and cerebrospinal fluid (CSF) secretion and flow.** Adapted from (Lehtinen et al. 2013).

The choroid plexus (CP) is constituted by a monolayer of choroid plexus epithelial cells located on a basement membrane. Under this monolayer of cells exists a stroma perfused with permeable fenestrated blood vessels, fibroblasts, and immune cells such as dendritic cells and macrophages (Figure 3). As such the CP forms a barrier between the blood and the CSF (BCSFB) (Falcão et al. 2012; Lun et al. 2015).

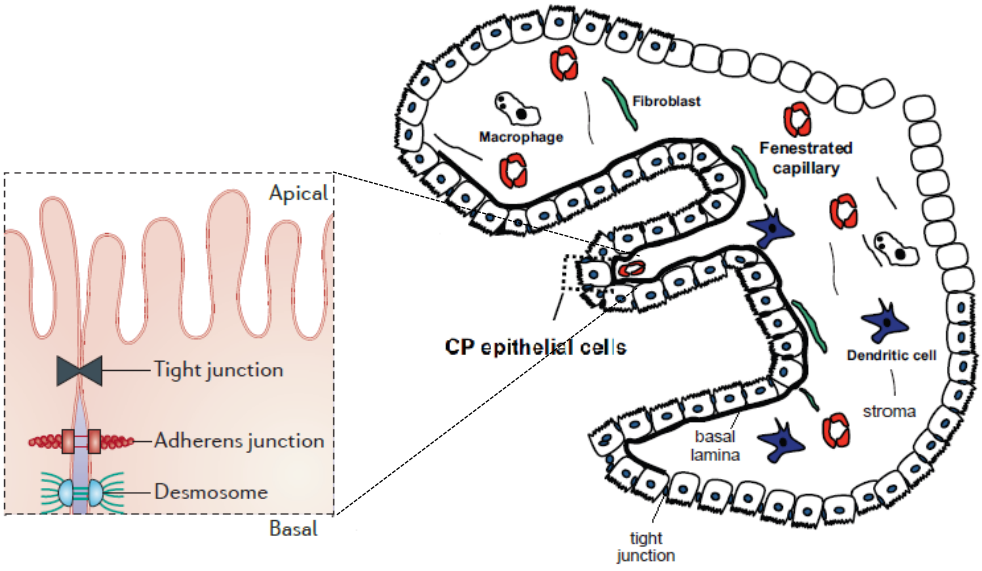

Figure 3 – **Morphologic representation of choroid plexus.** Adapted from (Falcão et al. 2012; Lun et al. 2015).

The CPEC are interconnected at the luminal membrane with tight junctions, adherents junctions (AJs) and desmosomes, that restrict the passage of different substances and pathogens between the blood and the CSF (Figure 3) (Damkier et al. 2013; Balusu et al. 2016).

CPEC have a large number of microvilli at the apical side (ventricle-CSF facing), and an extensive infolding at the basolateral side (stromal side), enabling a great interaction between the CP epithelium and CSF, and between the epithelium and stroma interstitial fluid, respectively (Santos et al. 2017).

The high capacity of synthesis of CP is demonstrated by the large number of mitochondria, Golgi apparatus, lysosome-like vesicles and smooth endoplasmic reticulum (Marques et al. 2013).

1.1.1.1 Functions

Besides its barrier function, the choroid plexus has many other relevant functions. CNS homeostasis depends directly from the different functions performed by CP: regulation of substances exchange between the blood and CSF; chemical surveillance; CSF secretion; synthesis and secretion of different substances, such as growth factors (GFs), vitamins, peptides and hormones; immune surveillance; neurogenesis, chemo surveillance, and the clearance of noxious compounds and metabolism waste products from the brain, including amyloid beta (Aß) (Santos et al. 2017). Some of these latter functions will be explained in the next sections, because of their relevance for the present work.

1.1.1.1.1 Cerebrospinal Fluid Production and Secretion

The choroid plexus, particularly the choroid plexus epithelium, is defined as a secretory tissue per excellence, responsible for producing the cerebrospinal fluid (Damkier et al. 2013). About 80% of the CSF is produced by the CP at a rate around 0,4 mL min^{-1} g $tissue^{-1}$ and the other 20% come from the interstitial brain fluid, which have a restricted relation with the blood-brain barrier. Notably, the total area of the CP surface is only about 0,1% of the BBB, demonstrating that CPE cells are one of the most efficient tissues in terms of secretory rate. Per day, the rate of CSF formation in humans is around 500 to 600 mL, but the CSF volume in a normal adult brain is 90-150 mL, suggesting that the total CSF volume is replaced three or four times in a day (Damkier et al. 2013). CSF has several functions in human brain, specially its protection during physical changes, and the capacity to enable exchanges between the CNS and the blood. Different substances pass between the blood to the brain such as glucose, amino acids, vitamins, growth factors, neurotrophins, hormones and free fatty acids, while toxins and waste products are expelled from the CNS to the blood, showing the importance of the CP-CSF system to physiological processes and maintenance of brain homeostasis (Johanson et al. 2011; Balusu et al. 2016). CSF formation that is enabled by capillary permeability and CPs epithelia, occurs in two different stages; passive filtration of fluid across the highly permeable endothelium and regulated secretion across the single layer of CP epithelium. This is regulated by membrane transporters within the epithelium, like the aquaporin 1 (AQP1) expressed at the apical membrane (CSF facing). In the same membrane, K^+/Cl^- co-transported is co-localized with Na^+/K^+-ATPase and the junction of these transporters can expel the water

from the cells to the CSF space (Brinker et al. 2014; Santos et al. 2017). CSF is secreted by CPs to the respective brain ventricle, where it contacts the ependymal epithelium and flows in a constant direction from the lateral ventricles to the fourth ventricle and beyond. When in the lateral ventricles, CSF flows through the Monro's foramina into the third ventricle, and then from the Sylvius aqueduct to the fourth ventricle. Here, the CSF leaves the ventricular system, through the Magendie's and Luschka's foraminas, to the subarachnoid space, where pia mater separates from the outer surface of the brain. The CSF returns to venous blood in brain sinuses via the arachnoid granulations, a central core that resembles the subarachnoid space and villi. The pressure gradient between the subarachnoid space and the venous sinus determines the reabsorption rate of CSF (Damkier et al. 2013).

1.1.1.1.2 Chemical Vigilance

As an important brain barrier, the CP has the capacity to monitor the CSF composition and control chemical exchanges between the blood and this brain fluid, enabling a correct concentration of substances in the brain. This might be of extreme importance for restraining the bioavailability of some drugs to the brain, thereby diminishing their efficacy against brain diseases. This restriction results from different mechanisms that control the cerebral extracellular fluid homeostasis (Ghersi-Egea et al. 2009). Previous microarray studies revealed that physiological pathways enabling the detection of chemicals, such as the taste and olfactory transduction pathways, and xenobiotics detoxification pathways are expressed in rat CPs (Quintela et al. 2013; Santos et al. 2017).

1.1.1.1.2.1 Taste Signalling

The taste transduction pathway was originally identified in taste buds in the mouth but an increasing number of studies have detected these taste receptors in non-oral tissues: in different types of cells in the airways (Tizzano et al. 2011), in the gastrointestinal duct (Depoortere 2014), in testis (Xu et al. 2013), in the kidney (Liu et al. 2015), in keratinocytes (Wölfle et al. 2015), in the thyroid gland (Clark et al. 2015) and has already been identified in CPEC, where it is functional (Tomás et al. 2016). These tissues where taste transductions are active, work as a barrier, so it seems that this receptor system acts as a sensor to assess body fluids' composition.

The binding of different substances to specific taste receptors in the taste buds leads to taste perception described as sweet, that identifies energy-rich nutrients as sugars and carbohydrates, sour, which is potentiated by acids, bitter, that warn for potentially noxious chemicals, salty, which allows Na^+ detection and umami that enables amino acids detection (Chaudhari & Roper 2010).

Responses to sweet, umami and bitter start with the binding of the tastant molecule to a G protein-coupled receptor (GPCR) family receptor. When the tastant molecule binds to the taste receptor originates a conformational change and leads to an activation of a series of

signal transducers as the G-protein gustaducin that activates a specific phospholipase C-beta2 (PLC-ß2) to enable inositol 1,4,5-triphosphate (IP_3). In its turn, IP_3 opens type 3 receptor ion channels (IP_3R3) leading to an increase of the intracellular Ca^{2+} levels which activate a taste-selective cation channel, the transient receptor potential channel M5 (TrpM5), depolarizing the cell. In salt or sour detection, the ion channels are directly opened. (Chandrashekar et al. 2006)

There are two different classes of taste GPCRs, the taste receptors type 1 (T1Rs) with T1R2 and T1R3 that responds to sweet and T1R1 and T1R3 responding to umami. Taste receptors type 2 (T2Rs) respond to bitter stimuli (Chandrashekar et al. 2006). There are studies which demonstrate the presence of T1R2 and T1R3 and their associated G-proteins in mammalians brain, more specifically in the hypothalamus, hippocampus and cortex (Xueying Ren, Ligang Zhou, Rose Terwilliger 2009). T2Rs were identified in CNS with a possible role to identify bitter compounds (Singh et al. 2011)

In CPs epithelial cells the presence of the mRNA and protein to type 1 member 1, 2 and 3 and type 2 member 109 and 40 taste receptors were confirmed as too the downstream signalling molecules as α-gustaducin, PLC-ß2, inositol IP_3 and TrpM5. Thus, taking as a principle that these receptors function as sensors in different barriers and with the confirmation of this presence in CP, it is likely that the taste pathway acts as one of the mechanisms by which this barrier surveys the CSF chemical composition (Tomás et al. 2016).

1.1.1.1.2.2 Clearance of Xenobiotics

There are evidences that drug detoxification mechanisms are present in the interface between the blood and the CSF. Due to the action of protein transporters, antioxidant mechanisms or drug metabolizing enzymes, the CP has the capacity to make the clearance of xenobiotics from the brain (Choudhuri et al. 2003; Ghersi-Egea et al. 2006).

This clearance involves three different phases. The first one which involves monoamine oxidases, epoxide hydrolases, NADPH-cytochrome P450 reductase, flavin-containing monooxygenases, and members of the cytochrome P450s family, leads to an enzymatic conversion of the xenobiotics into more hydrophilic metabolites, inactivating exogenous compounds as pesticides and carcinogenic molecules, increasing their susceptibility to phase II enzymes. In this second phase the enzymes as UDP-glucuronosyl transferases, sulfotransferases and glutathione S-transferases produce less toxic compounds and increase their polarity to enable the excretion by the urine and bile. In the last phase (III), several efflux transporters present in choroid plexus extrude the metabolism products (Ghersi-Egea et al. 1994; Strazielle et al. 2004; Ghersi-Egea et al. 2006; Ek et al. 2010). Moreover, the CPs have some antioxidant enzymes which inactivates potentially reactive and deleterious molecules resultant of phases I and II (Kratzer et al. 2013).

In microarrays studies of CPs were found the genes coding for phase I, phase II and phase III as well as antioxidant enzymes, proving the capacity of this barrier to do the xenobiotic´s clearance (Quintela et al. 2013; Santos et al. 2017).

1.1.1.1.2.3 Clearance of Amyloid Beta

An important cause of neurodegeneration in Alzheimer´s disease (AD) is the brain accumulation of amyloid beta as consequence of their overproduction and fail of different mechanisms as transport, metabolism and clearance (Kepp 2016).

The CP express some genes which are involved different processes from Aß production to its clearance as amyloid beta precursor protein (APP), beta-site APP-cleaving enzyme 1 and 2, nicastrin and presenilin 1 and 2 (Santos et al. 2017). Many of these enzymes are regulated by sex hormones (SH) which corroborates with the hypothesis that one of the possible causes to Alzheimer´s disease is the SH decline during the aging (Duarte et al. 2016).

1.1.1.1.2.4 Olfactory Signalling

Olfaction is an extremely important function to many species. It enables to explore their environmental composition, the food location, the territory recognition, the distinction between their conspecifics and predators and to avoid potentially harmful situations (Izquierdo et al. 2018). The olfactory system has the capacity to detect a lot of organic compounds with diverse chemical structures and properties through a series of mechanisms explained in the previous section (Du et al. 2013).

Olfactory receptors (ORs) are a type of transmembrane domain G protein-coupled receptor found in the olfactory sensory neurons (OSNs) across the olfactory epithelium, enabling the detection of different volatile odorants (Buck & Axel 1991). In vertebrates, the olfactory transduction pathway becomes activated when one of this volatile odorant binds to an OR and unleash the second messenger cascades of adenosine 3´,5´-cyclic monophosphate (cAMP) and inositol 1,4,5-trisphosphate signalling pathways. Previous evidences support that the most common activated pathway in mammals is cAMP by the stimulation of ORs with ligand binding, followed by the activation of olfactory specific G protein species as $G_{\alpha olf}$. This pathway generates an increase of intracellular cAMP by membrane adenylate cyclase 3 (AC3), leading to an increase of external Ca^{2+} influx by a cation-selective cyclic nucleotide-gated channel 2 (CNG2), and consequent membrane depolarization and generation of action potentials in OSNs (Figure 4) (Kang & Koo 2012). In fish species, such as *zebrafish* (*Danio rerio*), the binding of odorants activates phospholipase-C and originates diacylglycerol (DAG) and IP_3, which plays a role in membrane depolarization (Bruch 1996).

Evidences from electrophysiology experiments reported that murine CP has the ability to respond to polyamines stimuli, concluding that cAMP and phospholipase C-inositol 1,4,5-triphosphate signalling pathways are activated by this stimulation (Gonçalves et al. 2016).

The expression of olfactory receptors in different non-olfactory tissues such as testes, muscle, tongue, heart, brain, liver, spleen, pancreas, prostate, placent, lung, kidney, gastrointestinal tract and in the blood in human, mouse and in rat suggests that these receptors also play other physiological functions, including the detection of some molecules in body fluids (Kang & Koo 2012). Thus, CP may also be a potential sensor for CSF chemical surveillance (Santos et al. 2017).

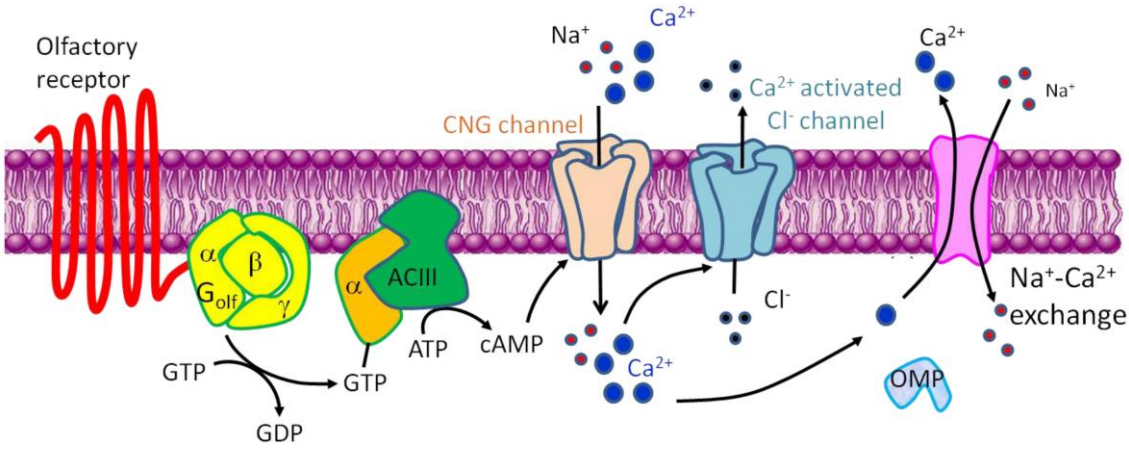

Figure 4 - **Olfactory signal transduction.** Adapted from (Kang & Koo 2012) Olfactory transduction is activated when a volatile odorant binds to an OR in the ciliary membrane, generating an increase of intracellular adenosine 3´,5´-cyclic monophosphate (cAMP) by membrane adenylate cyclase 3 (AC3), through a G protein ($G_{\alpha olf}$). This leads to an increase of external calcium (Ca^{2+}) influx by a cation-selective cyclic nucleotide-gated channel 2 (CNG2), followed by membrane depolarization by the Ca^{2+} activated chlorine (Cl^-) channel and generation of action potentials in OSNs. OR, olfactory marker protein (OMP), G_{olf} protein α-subunit ($G_{\alpha olf}$), and AC3 are known to be olfactory specific molecules. GTP- guanosine triphosphate; GDP- guanosine diphosphate; ATP- adenosine triphosphate; Na^+- sodium ion.

1.2 Trace Amine Associated Receptors

There are studies in mouse and fish which indicate that components of the “rotting flesh” odour as the polyamines can activate chemosensory receptors present in the olfactory epithelium, named trace amine-associated receptors (TAARs) (Pacifico et al. 2012; Hussain et al. 2013; Dieris et al. 2017).

Trace amines are primary amines which are synthesis or metabolism products of their monoamine precursors. Tryptamine, ß-phenylethylamine, para-/meta-tyramine, para-/meta-octopamine synephrine, 3-iodothyronamine and 3-methoxytyramine can be found in human brain at concentrations around 100 times lower than the most common monoamines, dopamine, norepinephrine and serotonin (Berry 2004; Grandy 2007; Sotnikova et al. 2010). There are evidences which support that TAs levels are altered in several neuropsychiatric disorders as attention deficit, depression, hyperactivity disorder, schizophrenia and Parkinson´s disease, suggesting the role of these amines in the monoaminergic system (Branchek & Blackburn 2003; Burchett & Hicks 2006). Trace amine associated receptors were discovered in 2001 and initially proposed to bind low abundance neurotransmitters, the trace

amines (Borowsky et al. 2001; Bunzow et al. 2001; Lindemann & Hoener 2005). This discovery of a new family of receptors opens a lot of new perspectives in different areas, from the biochemistry to the cell biology, with impact in physiology, pharmacology and pathophysiology of different organs as brain, thyroid gland, OSNs and others (Zucchi et al. 2006). They are part of the rhodopsin-like GPCRs with 7 transmembrane domains and short N and C-terminals, initially recognized as receptors that can identify trace amines. These are now considered as key targets in drug development. TAARs act as olfactory receptors, and are evolutionarily conserved throughout diverse vertebrate species. There are 112 types of full-length TAARs in zebrafish, 17 in rat, 15 in mouse and 6 in macaque. In human, the 6 types of TAAR genes (1, 2, 5, 6, 8 and 9) and 3 pseudogenes (3, 4 and 7 subtypes) are located at chromosome 6 at band q23.1 (Figure 5), and are expressed within the sensory neurons in the olfactory cilia and in axons. These receptors are also expressed in other different brain regions, and other human tissues (Table 1) (Liberles 2015; Berry et al. 2017). Based on studies done in rodents, primate and fish, all of the TAARs except TAAR1 function as olfactory receptors expressed in the olfactory epithelium, coupled to G_{olf} protein regulating cAMP accumulation. (Liberles & Buck 2006; Hussain et al. 2009; Horowitz et al. 2014). TAARs also present homology with biogenic amine receptors, recognizing amines through a salt bridge with a conserved transmembrane three aspartic acid, $Asp^{3.32}$, a motif which is retained in all of human TAARs and consequently suggesting that these receptors would retain capacity to recognize amines (Liberles 2015).

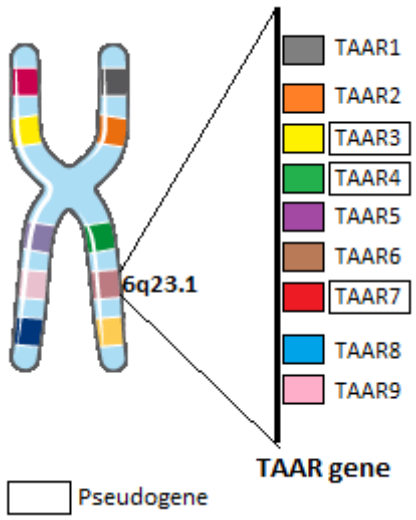

Figure 5 – **Chromosome location of human TAAR genes.** TAAR genes are located at chromosome 6 at q23.1 band. There are 9 different types of TAARs in humans, however only 6 are functional, 3 are pseudogenes.

Table 1 - **Expression and functions of trace amine associated receptors**. h- human; r- rat; z- *zebrafish*; ST- signal transduction; ?- not confirmed, only evidences.

TAARs	Species/Tissue	Functions	Ligands/Signal transduction	References
TAAR1	**h**: brain (ventral tegmental area, dorsal raphe, amygdala, striatum, hypothalamus, frontal cortex), spinal cord, pancreatic ß-cells, stomach, intestines, leukocytes and human breast cancer tissue. **m**: pancreatic ß-cells, stomach, intestines and leucocytes **r**: heart, pancreatic ß-cells, stomach, intestines and testis **z**: olfactory epithelium	Modulation of dopaminergic, serotonergic, and glutamatergic neurotransmission. Regulation of reward circuits, limbic network, cognitive processes, and mood states. Regulation of hormone release, glucose levels and body weight.	Trace amines, others; ST: G_s, ß-arrestin 2, GirK channels, possible constitutive activity	(Borowsky et al. 2001) (Bradaia et al. 2009) (Ito et al. 2009) (Revel et al. 2011) (Gozal et al. 2014) (Liberles 2015) (Espinoza et al. 2015) (Vattai et al. 2017)
TAAR2	**h:** olfactory epithelium, intestines, heart, testes, leukocytes, B-cells, granulocytes, monocytes, NK-cells, and T-cells **m:** gastrointestinal tract (duodenal mucosal cells) **r:** heart and testis	Olfaction; Leukocyte regulation; A single nucleotide polymorphism (SNP) nonsense mutation was detected in TAAR2 in schizophrenia patients	Primary amines? ST: G_{olf},G_i?	(Chiellini 2007) (Ito et al. 2009) (Chiellini et al. 2012) (Ferrero et al. 2012) (Liberles 2015) (Malki et al. 2015)
TAAR3	**m:** olfactory epithelium **r:** spinal cord **h** (pseudogene)	-	Isopentylamine; ST: G_s	(Borowsky et al. 2001) (Lindemann & Hoener 2005) (Lindemann et al. 2005) (Liberles 2015)
TAAR4		-	2-phenylethylamine;	(Borowsky et al. 2001)

	r: brain (substantia nigra/ventral tegmental area, locus coeruleus, and dorsal raphe) h (pseudogene)		Tyramine	(Lindemann et al. 2005) (Liberles 2015)
TAAR5	**h:** olfactory epithelium, brain restricted, spinal cord, intestines, testis, leukocytes and B-cells **m:** brain (amygdala, arcuate nucleus, and ventromedial hypothalamus) **r:** spinal cord, testis, intestines	Olfaction	Trimethylamine; ST: G_{olf}, G_s, $G_{q/11}$,$G_{12/13}$	(Chiellini et al. 2012) (Wallrabenstein et al. 2013) (Gozal et al. 2014) (Kubo et al. 2015) (Liberles 2015) (Dinter, Mühlhaus, Jacobi, et al. 2015) (Dinter, Mühlhaus, Wienchol, et al. 2015)
TAAR6	**h:** brain (amygdala, basal ganglia, frontal cortex, hippocampus, substantia nigra), olfactory epithelium, intestines, testis, leukocytes, kidney **m:** duodenal mucosal cells **r:** spinal cord and testis	Olfaction; Significant associations with bipolar and schizophrenic disorders.	Diamines, tertiary amines? ST: G_{olf}	(Borowsky et al. 2001) (Duan et al. 2004) (Ito et al. 2009) (Chiellini et al. 2012) (Ferrero et al. 2012) (Gozal et al. 2014) (Li et al. 2015) (Liberles 2015)
TAAR7	**m:** olfactory epithelium **h** (pseudogene)	-	N,N-dimethylalkylamines	(Lindemann et al. 2005) (Liberles 2015)

TAAR8	**h:** olfactory epithelium, brain (amygdala, astroglia) leukocytes, stomach, intestines, heart, testes, lungs, spleen, kidney, muscle **m:** astroglia, leukocytes, heart, intestines, kidney, lung, muscle, spleen, stomach and testis **r:** spinal cord, brain (cortex, cerebellum)	Olfaction; In astroglial cells are up-regulated following stimulation with lipo-polysaccharides strengthened the assumption of a TAAR8 distinct role in the brain	N-methylpiperidine; ST: G_{olf}, G_i	(Borowsky et al. 2001) (D´Andrea 2003) (Nelson 2007) (Chiellini et al. 2012) (Gozal et al. 2014) (Mühlhaus et al. 2014) (Liberles 2015)
TAAR9	**h:** olfactory epithelium, pituitary gland, spinal cord, intestines, spleen, skeletal muscle, leukocytes **m:** duodenal mucosal cells **r:** spinal cord	Olfaction	N-methylpiperidine; ST: G_{olf}	(D´Andrea 2003) (Vanti et al. 2003) (Regard et al. 2008) (Ito et al. 2009) (Gozal et al. 2014) (Liberles 2015)
TAAR13c	**z:** olfactory epithelium (OSNs)	Olfaction	Cadaverine	(Hussain et al. 2013) (Liberles 2015)

These differences observed between different species suggest the role of TAAR genes in the adaptation process during evolution suggesting too their linkage with some diseases probably related with different lifestyles and body functions in humans and in other species (Olson, Maynard V.; Varki 2003). The evolution pattern of the TAARs gene family is characterized by a specific phylogenetic clustering. Like ORs, the TAARs present an evolutionary conservation from fish to humans (Gloriam et al. 2005; Lindemann et al. 2005). There are some findings which raise the hypothesis that TAARs have been conserved owing to a improved ability to enable innate responses as avoidance (Mitchell & Smith 2001; Ferrero et al. 2011; Dewan et al. 2013; Hussain et al. 2013; Qian Li et al. 2013)

TAARs signalling present sequence similarities with ORs but they are not phylogenetically related with canonical ORs or another different type of chemosensory receptors. TAARs also activate cAMP pathways when binding an olfactory amine (Nei et al. 2008; Liberles 2015). The number of TAAR genes is smaller when compared with the number of ORs genes evidencing the importance of the TAARs, because in vertebrate species, a low copy number in the gene families is interconnected with their importance in biochemical functions (Nei et al. 2008).

In the last years, the zebrafish emerged as an important model to understand the olfaction process in vertebrates because of their similarity in the olfactory process (Yoshihara 2008). In the sea, the zebrafish tissue decay originates a strongly repulsive odour of cadaverine which causes a repulsive response in this species (Figure 6) (Hussain et al. 2013). As in mammals, in this fish species, the TAARs act as olfactory receptors. TAARs are a large family of receptors in zebrafish in which 112 receptors are encoded by its genome (Liberles & Buck 2006; Hussain et al. 2009). There are studies showing that TAAR13c binds cadaverine, that exhibits a strong response to this diamine (Hussain et al. 2013).

TAAR 13c is a diamine receptor with distinct recognizing capacity when compared with other biogenic amine-activated GPCRs, found in olfactory sensorial neurons of zebrafish. It has affinity to cadaverine, an odour produced through lysine decomposition product by bacteria and characterized as a medium-sized and odd-chained diamine. OSNs that express TAAR13c are activated with low cadaverine concentrations with high specificity, suggesting their importance in the neuronal processing pathway through a parallelism between linking cadaverine and an aversive innate response (Figure 6) (Hussain et al. 2013; Li et al. 2015; Liberles 2015; Dieris et al. 2017).

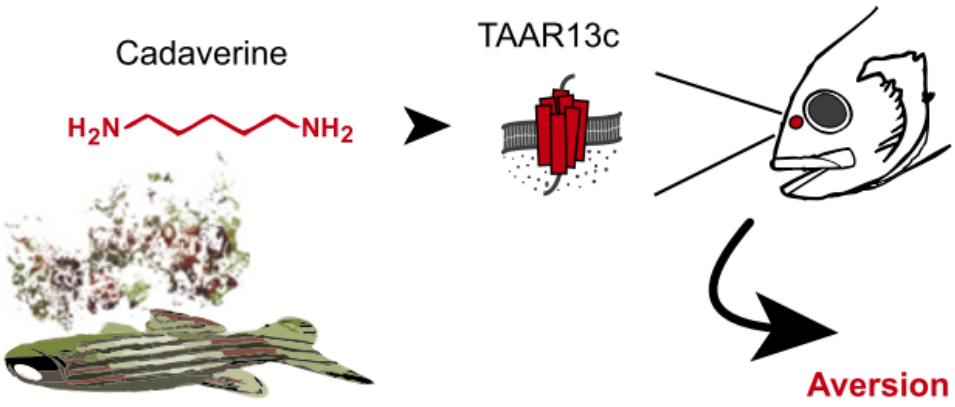

Figure 6 – **Graphical summary of key findings to aversion to cadaverine by *zebrafish*.** Adapted from (Hussain et al. 2013).

It has been demonstrated previously that CP cells and explants respond to polyamines, cadaverine, spermine, spermidine and putrescine. The response to spermine is reduced when protein G_{olf} is silenced (Gonçalves et al. 2016). So, either the odorant signalling pathway or the TAAR signalling pathway could be involved.

Taking in consideration that TAAR13c binds to cadaverine in zebrafish we looked at it homologous in the human genome databases. We found that the human variants of TAARs that show the highest homology to TAAR13c (Gene ID: 100034378) and more abundance in human tissues are TAAR1 (Gene ID: 134864), 2 (Gene ID: 9287) and 5 (Gene ID: 9038) (Hussain et al. 2013).

TAAR 1 is a class A GPCR, a member of the rhodopsin-type superfamily, with 339 amino acids and was the first TAAR to be deorphanized in rat brain and initially it was demonstrated that is activated by tyramine and ß-Phenylethylamine (ß-PEA) and displays low affinity for tryptamine, octopamine, and dopamine (DA). It is located at the intracellular space possibly associated with a yet unknown membrane component in neurons, glial cells and in peripheral tissue. It is expressed at different levels in mammal's different tissues as in human major monoaminergic regions, such as ventral tegmental area (VTA) and dorsal raphe, and their projections, including amygdala, striatum, hypothalamus and frontal cortex, in the spinal cord, pancreatic ß-cells, stomach, intestines, leukocytes and human breast cancer tissue (Borowsky et al. 2001; Stäubert et al. 2010; Revel et al. 2011; Chiellini et al. 2012; Liu et al. 2015; Khan & Nawaz 2016; Berry et al. 2017; Vattai et al. 2017). The expression of this human receptor is poor at the plasma membrane, possibly due to the absence of N-terminal glycosylation sites, however, there is little information about their expression in the human central nervous system (Berry et al. 2017). TAAR1 discovery attracted the attention because it is activated not only by the trace amines as tyramine, tryptamine, octopamine, 2-phenylethylamine, thyronamines and other amines, but also by psychoactive chemicals as amphetamines. This suggests its importance as a negative modulator of the dopaminergic

system influencing the dopamine, serotonin and potentially norepinephrine neurotransmission and acting as a promising target for the treatment of neuropsychiatric disorders treatment. Table 2 presents the half maximal effective concentration (EC_{50}) for the trace amines to TAAR1 (Tan et al. 2009; Khan & Nawaz 2016; Berry et al. 2017).

TAAR2 is also a G protein-coupled receptor whose gene contains two exons and codifies to a 351 amino acids protein. Its secondary structure presents 7 transmembrane domains (Khan & Nawaz 2016; Berry et al. 2017). It is expressed in the olfactory epithelium, cerebellum, intestines, heart, testes and leucocytes, in different cells of the gastrointestinal system in human, mice, and in rat (Chiellini 2007; Ito et al. 2009; Chiellini et al. 2012; Khan & Nawaz 2016; Berry et al. 2017). Based on evolutionary mapping, there are evidences that TAAR2 binds to primary amines (Ferrero et al. 2012).

TAAR5 is the most conserved olfactory TAAR subtype between all the mammalian species. Its gene has 1014 base pairs, only an exon and codifies to a 337 amino acids protein. It is expressed at the olfactory epithelium, brain (amygdala, arcuate nucleus, and ventromedial hypothalamus), spinal cord, intestines, testes and leucocytes in humans, mouse and rat (Chiellini et al. 2012; Gozal et al. 2014; Dinter, Mühlhaus, Wienchol, et al. 2015; Kubo et al. 2015; Khan & Nawaz 2016; Berry et al. 2017). It binds to trimethylamine and it is coupled to the G_s cascade, the $G_{q/11}$ cascade and $G_{12/13}$ dependent MAP kinase pathways (Wallrabenstein et al. 2013; Dinter, Mühlhaus, Wienchol, et al. 2015; Dinter, Mühlhaus, Jacobi, et al. 2015).

The TAAR6 which is also an olfactory TAAR probably associated with trace amines (Khan & Nawaz 2016; Berry et al. 2017). It is expressed in the olfactory epithelium, brain, more specifically in amygdala, basal ganglia, frontal cortex, hippocampus and substantia nigra, spinal cord, intestines, testes, leucocytes and kidney in human, mouse and rat (Borowsky et al. 2001; Duan et al. 2004). (Borowsky et al. 2001; Duan et al. 2004; Ito et al. 2009; Chiellini et al. 2012; Gozal et al. 2014).

TAAR8 is a G_i protein coupled receptor present in olfaction processes and it is encoded by a 1029 base pairs gene (Berry et al. 2017). It is expressed in the olfactory epithelium, amygdala, astroglia, cortex, cerebellum, spinal cord, leucocytes, stomach, intestines, heart, testes, lungs, spleen, kidney and muscle, in humans, mouse and rat (Borowsky et al. 2001; D´Andrea 2003; Nelson 2007; Chiellini et al. 2012; Gozal et al. 2014).

Finally, TAAR9 which is expressed in olfactory epithelium, spinal cord, intestines, spleen, skeletal muscle, pituitary gland and leucocytes in humans, mouse and rat (D´Andrea 2003; Vanti et al. 2003; Regard et al. 2008; Ito et al. 2009; Gozal et al. 2014), is codified by a 1047 base pairs gene with only an exon (Berry et al. 2017).

Table 1 summarizes the information about TAARs expression, functions, ligands and signalling pathways.

Table 2 - **Pharmacology of human trace amine associated receptor 1** (Lindemann et al. 2005; Cöster et al. 2015; Simmler et al. 2016).

Human Trace Amines	Human TAAR1 EC_{50}
ß-Phenylethylamine	0.26 µM
p-Tyramine	0.99 µM
Octopamine	10 µM
Tryptamine	21 µM
3-Iodothyronamine	1.7 µM
Trimethylamine	Not determined

1.2.1 Trace Amine Associated Receptor 1 Transduction Pathway

As TAAR1 is the target of this study, in this section the transduction pathway for this receptor is explained in detail.

At the olfactory system, the expressed TAARs are co-expressed with olfactory guanine nucleotide-binding protein, G protein, (G_{olf}) and consequently linked to a cAMP accumulation as occurs in the ORs transduction pathway (Liberles & Buck 2006). As an exception, TAAR1, is not considered a human olfactory TAAR because of its absence of expression in the human olfactory epithelium. It is coupled to a G_s-protein and in addition to triggering intracellular cAMP production via adenylyl cyclase activation, it also involves an independent G protein ß-arrestin 2 cascade (Harmeier et al. 2015; Pei et al. 2016; Berry et al. 2017). An example to elucidate TAAR1 transduction pathway is dopamine secretion by neurons where this G-protein independent, ß-arrestin2 dependent pathway involves the protein kinase B/glycogen synthase kinase 3 (GSK-3) ß signalling cascade. Dopamine receptors (DR) are also GPCRs and form heterodimeric complexes with TAAR1, moreover, interaction of TAAR1 with dopamine receptors reduces ß-arrestin 2 recruitment to DR and their capacity to elevate cAMP production, whereas ß-arrestin 2 signalling is enhanced, leading to a reduced GSK-3 activation. The phosphorylation of the dopamine transporters (DAT) through TAAR1 activation by its stimulation leads to DAT internalization, which results in a reduced uptake of DA (Figure 7) (Pei et al. 2016; Asif-Malik et al. 2017).

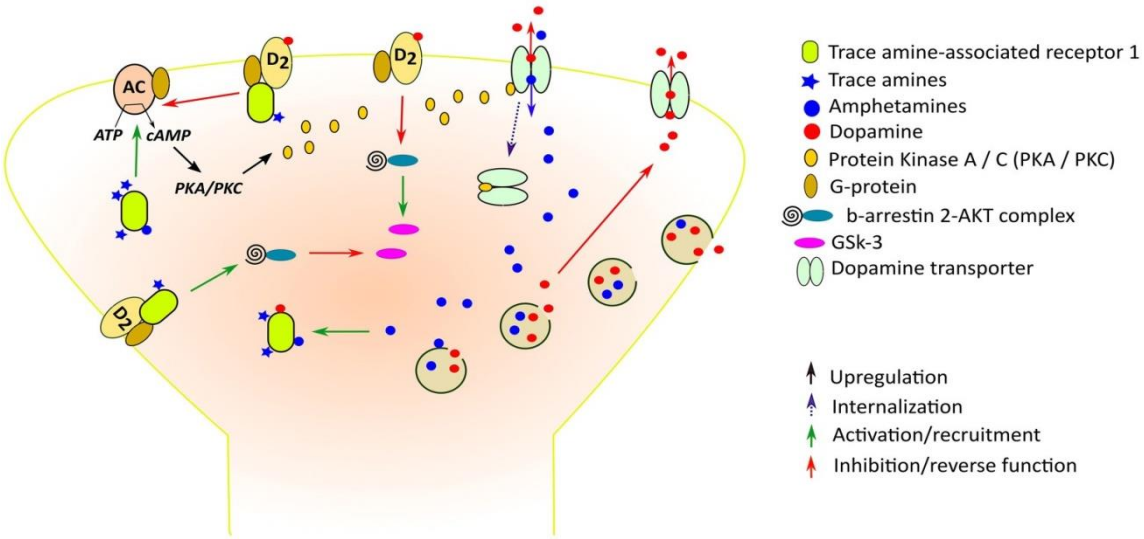

Figure 7 – **Trace amine associated receptor 1 (TAAR1) at a DA synapse.** Adapted from (Pei et al. 2016). At the presynaptic neurons the amphetamines enter through competitive reuptake of the dopamine transporters (DAT) and by diffusion through presynaptic membranes, resulting in dopamine (DA) release by reverse transport through the DAT and by vesicular monoamine transporter-mediated exocytosis. TAAR1 is activated by amphetamines and endogenous trace amines leading to an adenylate cyclase activation and a consequent downstream cascade by protein kinase A/protein kinase C (PKA/PKC). TAAR1 also signals by G-protein independent, ß-arrestin 2 dependent pathway involving protein kinase B/glycogen synthase kinase 3 (GSK-3) ß signalling cascade. In D2R case, ß-arrestin enhance the interaction between AKT and protein phosphatase 2A resulting in AKT activation and a consequent activation of GSK-3. As GPCRs, when D2s binds to TAAR1 form heterodimeric complexes which reduce ß-arrestin 2 recruitment to D2R and its ability to decrease cAMP production and resulting in a reduction of GSK-3 activation. DAT phosphorylation by TAAR1 stimulated activation leads to a DAT internalization that results in a reduction in DA uptake.

1.3 Polyamines

Polyamines (PAs) are polycations which appear naturally in cells, being essential small aliphatic hydrocarbon chains with one or more amine groups which interact with negative charged molecules such as deoxyribonucleic acid (DNA), ribonucleic acid (RNA) or proteins (Minois et al. 2011; Perez-Leal & Merali 2012; Pegg 2016; Gevrekci 2017). At physiological conditions, during growth, survival and proliferation, cells synthesize diverse polyamines, like putrescine (1,4-diaminobutane), spermine (N,N'-bis(3-aminopropyl-1,4-butanediamine)), spermidine (N-(3 aminopropyl)-1,4-butadiamine) (Yatin 2002). Cadaverine (1,5-pentanediamine) is a diamine and a death-associated odour produced through lysine catabolism catalysed by microbe-mediated decarboxylation of lysine by lysine decarboxylase enzyme (Mietz JL 1978; Tabor & Tabor 1985; Tomar et al. 2013). A natural source of cadaverine is the decaying of animal tissues as the example with more relevance to this work, the zebrafish, where this polyamine is produced and consequently dissolved in the sea water where later it can be detected by the TAAR13c expressed in the olfactory epithelium of this fish species (Hussain et al. 2013).

In the CSF of adult brain, under physiological conditions, PA concentrations are around 0.13±0.02 nM for putrescine, 0.14±0.01 nM to spermine, 0.12±0.01 nM to spermidine and 2.12±1.48 nM to cadaverine (Ekegren & Gomes-Trolin 2005; Paik et al. 2010).

PAs are closely related with neuronal cell biochemical activity at different points, such as interaction with neurotransmitter receptors, ion channels, regulation of substances in degenerating cells and protection of neuronal cells from oxidative stress. So, PAs are also deregulated in different brain diseases like Alzheimer's, and Parkinson's (PD) and amyotrophic lateral sclerosis (ALS), where putrescine levels are decreased and spermine and spermidine levels are increased (Yatin et al. 1999; Gomes-Trolin et al. 2002; Antony et al. 2003; Ramani et al. 2014).

Polyamine´s homeostasis in cells is enabled by a strict balance between amine synthesis, uptake and degradation, and their content is controlled by key enzymes in their biosynthesis pathway (Perez-Leal & Merali 2012).

1.3.1 Biosynthesis and Catabolic Pathways

There are three different sources of polyamines in the organisms: food intake, cellular synthesis and microbial synthesis in the gut. Different amino acids, like arginine, ornithine, methionine and lysine, are known as precursors of polyamines, and PA biosynthesis is controlled by three critical enzymes: Spermidine/spermine N´-acetyltransferase (SSAT), ornithine decarboxylase 1 (ODC1), S-adenosylmethionine decarboxylase (SAMdc or AMD1) and lysine decarboxylase (LDC). They have a half-life around an hour and are regulated by a multiple step process of their synthesis and degradation (Minois et al. 2011; Campilongo et al. 2014; Ramani et al. 2014).

Arginase, a mitochondrial enzyme, produces ornithine from arginine, and then the ODC1 decarboxylates ornithine to produce putrescine, the simplest polyamine (Minois et al. 2011). A parallel mechanism is known for spermine and spermidine, which have the same precursor decarboxylated AdoMet (DcAdoMet). L-methionine is converted into S-adenosyl-L-methionine (AdoMet). This last one is decarboxylated to DcAdoMet, and then used as a donor of an aminopropyl group either to putrescine by spermidine synthase, to produce spermidine, or to spermidine to produce spermine by spermine synthase (Figure 8) (Perez-Leal & Merali 2012; Gevrekci 2017). Antienzyme 1 (Azin1) can be linked to ODC1 in peroxisome to enable its degradation, inhibiting PA biosynthesis (Minois et al. 2011).

Putrescine can be synthetized again trough conversion of superior polyamines, spermine and spermidine. These two last polyamines are acetylated by SSAT, using Acetyl Co-A as donor, and go to the peroxisome where they are oxidized by the polyamine oxidase (PAO) (Figure 7). On the other hand, acetylated polyamines can be excreted out of the cells (Minois et al.

2011; Perez-Leal & Merali 2012; Ramani et al. 2014). Spermine oxidase (SMO) can convert spermine in spermidine in the cell cytoplasm (Minois et al. 2011).

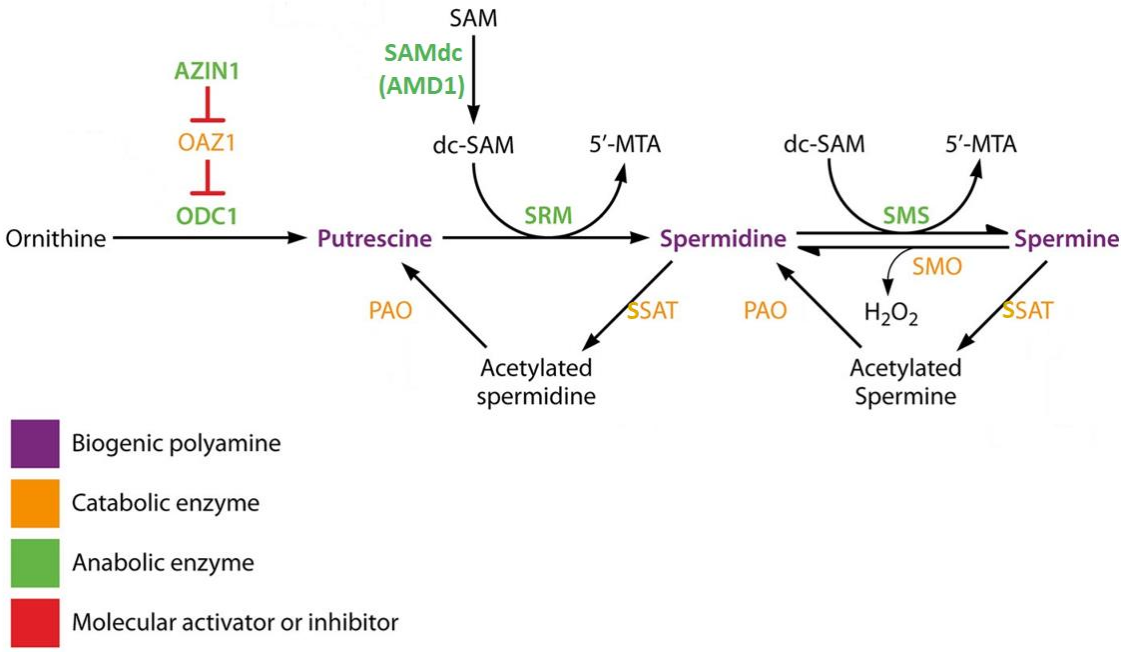

Figure 8 – **Polyamine biosynthesis and catabolism pathway**. Adapted from (Mounce et al. 2017). AZIN1- antienzyme 1; AMD1- S-adenosylmethionine decarboxylase; Oaz1- ornithine decarboxylase antienzime 1; ODC1- ornithine decarboxylase 1; PAO- polyamine oxidase; SMO- spermine oxidase; SMS- spermine synthase SRM- spermidine synthase; SSAT- spermidine/spermine N´-acetyltransferase.

Cadaverine is synthetized through lysine catabolism catalysed by microbe-mediated decarboxylation of lysine by lysine decarboxylase enzyme (Mietz JL 1978; Tabor & Tabor 1985; Tomar et al. 2013; Campilongo et al. 2014). There are studies which showed evidences that cadaverine is synthetized in mouse intestines through lysine decarboxylation by bacteria from the intestinal flora. However, studies performed by the same authors showed that cadaverine is produced in the mouse brain but this biosynthesis is not through bacterial decomposition (Stepita-Klauco & Dolezalova 1974; Schmidt-Glenewinkel et al. 1977). After a literature search no studies describing the origin of brain cadaverine were found, and it is likely that it remains unknown.

1.3.2 Functions

The biological roles of polyamines result from the interaction between this polycationic molecules and polyanionic molecules like DNA, RNA and phospholipids. Thus, PAs have an important role in many of the cellular processes, including cell growth, proliferation, differentiation, transcription, translation, regulation of ion channels, enzyme activities and response to the oxidative stress. As a consequence of the interaction with DNA and cellular proliferation, high levels of PAs are found in some diseases, like cancer and neuronal diseases (Minois et al. 2011; Perez-Leal & Merali 2012). It was shown that putrescine levels in red

blood cells are decreased in patients with Parkinson´s disease and amyotrophic lateral sclerosis, instead spermine and spermidine which is increased in both sets of patients, however there is no correlation between the changes in these polyamines levels and the disease severity (Gomes-Trolin et al. 2002).

Other studies showed that the accumulation of the Aß peptide and the consequent oxidative stress, responsible for Alzheimer´s disease, is prevented by polyamines through their metabolism upregulation (Yatin et al. 1999)

Antony *et al*. reported that spermine, spermidine and putrescine levels increased the aggregation of α-synuclein, a protein responsible for the Lewy body´s formation in Parkinson´s disease (Antony et al. 2003). Some evidences showed that spermine was proved to increase the ischemic neuronal injury in rodent model of ischemia (Bo Duan et al. 2011). On the other hand in a frog model of epilepsy it was demonstrated that putrescine is neuroprotective through its conversion into gamma-aminobutyric acid (GABA) (Bell et al. 2011).

As described in a previous section, the CPEC are interconnected at the luminal membrane with tight junctions, adherents junctions and desmosomes, that restrict the passage of different substances and pathogens between the blood and the CSF (Damkier et al. 2013; Balusu et al. 2016).

Polyamines have also a role in the formation of epithelial cell junctions through their role in the expression of E-cadherin, a key protein to AJs. Polyamines are responsible for regulating the transcription mechanism of E-cadherin gene and consequently modulating the E-cadherin stability in epithelial cells. The synthesis and stability of occludin and the formation of tight-junctions, is also polyamine dependent (Wang 2005; Ramani et al. 2014). They have also a role in the modulation of the signal transduction pathways. Has been shown that spermidine exerts effects in kinase signalling, in the modulation of phosphoinositide 3-kinase/protein kinase B (PI3K/AKT) signalling pathway. Polyamines as spermine stimulate the kinase A activity and putrescine and spermidine stimulate the tyrosine kinase-mediated phosphorylation of proteins (Bachrach et al. 2001; Pegg 2013; Rajeeve et al. 2013). As these signalling pathways are involved in the signalling transduction mechanisms of the TAARs, is possible to predict a role of these substances in these receptors functions.

Chapter 2

2. Aims

2. Aims

A previous study performed by our research group showed that rat choroid plexus cells are capable to detect polyamines and trigger a Ca^{2+} response when stimulated. These responses are diminished when G_{olf} is silenced. These findings suggest that the olfactory transduction pathway or TAAR signalling can be deployed by polyamines constituting a chemical surveillance mechanism of CP, contributing for brain homeostasis.

Thus, the main objectives of this project were:

i) To identify the receptors that respond to polyamines in humans, based on the homology with fish species where these have been identified;

ii) To analyse the metabolic pathway of polyamine synthesis and degradation in human CP cells.

Chapter 3

3. Materials and Methods

3. Materials and Methods

3.1 Data Base Search

To identify which human TAAR presents more percentage of homology with zebrafish TAAR13c, a BlastX (NCBI) search was done using the FASTA sequence for TAAR13c which was compared with human (*homo sapiens*) genome.

A search in the Gene Expression Omnibus data base was done to see which of these TAARs were the most expressed in human tissues.

3.2 Cell Culture

The human malignant choroid plexus papilloma cell line (HIBCPP) was used in this work, since it has the barrier characteristics as well as transport properties (Bernd et al. 2015) essential to this study. Cells were cultured with DMEM/F12 (Dulbecco's Modified Eagle Medium: Nutrient Mixture F-12; PanBiotech) containing 10% fetal bovine serum (FBS, Biochrom AG), 1% penicillin-streptomycin antibiotic (Sigma-Aldrich) and 5 µg/mL insulin (Sigma-Aldrich), and incubated at 37ºC and 5% carbon dioxide (CO_2) in an AutoFlow DHD CO_2 Air Jacketed Incubator (NuAire). Culture medium was changed every 2-3 days.

3.2.1 Cells Passage

To ensure the HIBCPP cell line expansion and prevent cell death, cells were trypsinized always when 80-90% of cellular confluence was reached. Briefly, the culture medium was removed and cells were washed with phosphate-buffered saline (PBS), followed by incubation at 37ºC with trypsin-ethylenediaminetetracetate (trypsin-EDTA) 0.25% solution until cell detachment. Trypsin action was then stopped by adding an equivalent volume of culture medium, cells were resuspended and transferred to a 50 mL falcon tube, followed by centrifugation during 10 minutes at 500 rpm. Finally, the pellet was resuspended in culture medium and the culture was established as described before.

3.2.2 Cell Counting

To count the cells, equivalent volumes of cell suspension and trypan blue 0.4% solution were taken, followed by homogenization, and 10 µL were transferred to a Neubauer chamber. The number of cells was estimated using the following expressions:

$$Cells/mL = mean\ of\ quadrants \times 2 \times 10^4 \times mL$$

$$Total\ number\ of\ cells = Cells/mL\ \times cells\ resuspension\ volume$$

3.2.3 Cells Freezing and Thawing

As described before, cells were trypsinized, resuspended in complete DMEM/F12 medium supplemented with 30% FBS and 10% DMSO (Dimethyl sulfoxide) to prevent crystals formation and consequent cell lysis during the freezing, and stored at -20ºC, -80ºC and finally in liquid nitrogen. To thaw, cells were resuspended in complete DMEM/F12 medium, centrifuged during 10 minutes at 500 rpm, and cultured as described before.

3.3 Total RNA Extraction and Quantification

The total RNA extraction was performed using 1 mL TRIzol® reagent (Sigma-Aldrich)/10 cm^2 culture area, followed by 5 minutes incubation at room temperature, enabling the complete nucleoprotein complex dissociation. After this step, 200 µL chloroform/mL TRIzol® were added and the sample was homogenized by inversion, followed by an incubation period of 10 minutes at room temperature, and centrifuged at 12000 g and 4ºC for 15 minutes. After centrifugation, the initial solution was separated into three phases: at the bottom of the tube was obtained the organic phase (pink colour) containing the proteins and residues of phenol and chloroform; the interface containing the DNA (white); and the aqueous phase (transparent) containing the RNA. The aqueous phase was transferred into a new 1.5 mL tube to which were added 500 µL of isopropanol/mL TRIzol®, followed by homogenization by inversion to allow RNA precipitation. After 10 minutes of incubation at room temperature and centrifugation at 12000 g and 4ºC for 10 minutes, supernatant was discarded and a RNA pellet was obtained. RNA pellet was washed with 500 µL of 75% ethanol in diethylpyrocarbonate water (DEPC), centrifuged at 7500 g for 5 minutes at 4°C, and the supernatant was discarded. Finally, the RNA was resuspended in DEPC water and stored at -80ºC.

The total RNA integrity was determined by electrophoresis in an 1% agarose gel stained with GreenSafe (NZYTech). Samples were prepared by adding 8 µL of DEPC water and 1 µL of loading buffer to 1 µL of sample. Gel was visualized using a transilluminator UVITEC. RNA quality was confirmed by the visualization of two bands of ribosomal RNA (rRNA), 18S and 28S, the last one presenting about the double of 18S intensity.

A nanophotometer (Nanophotometer™, Implen) was used to quantify the RNA. The purity degree was measured using the absorbances at 260 and 280 nm ratio. RNA is considered pure when the A_{260}/A_{280} ratio is between 1.8 and 2.1.

3.4 cDNA Synthesis

Complementary DNA (cDNA) was obtained using a reverse transcriptase enzyme that converts an RNA chain into a double cDNA chain.

To remove possible existing genomic DNA from the extracted RNA, a DNase I treatment was performed (DNAse I kit; Sigma-Aldrich). Briefly, per µg of RNA were added 1 µL of reaction

buffer 10X, 1 µL DNAse I (1U/µL) and H_2O DEPC until a final volume of 8 µL. Samples were placed on a thermocycler (Multigene Optimax Labnet) and incubated for 15 minutes at 37ºC. After that, 1 µL of STOP solution (EDTA 50 mM) was added, cheating Ca^{2+} and Mg^{2+} cations and consequently inactivating DNAse I, through incubation during 10 minutes at 70ºC.

The reverse transcription was then performed by preparing two mixes for each sample. The MIX1 containing 2 µL of random primers and 1 µL of deoxyribonucleotides triphosphate (dNTPs) per reaction was added to each RNA microtube previously treated with DNase I, followed by incubation on a thermocycler during 5 minutes at 65ºC. A MIX2 was prepared with 2 µL of RT buffer and 1 µL of MMLV-RT enzyme (NZYTech) and added to each microtube, followed by 50 minutes at 37ºC and 15 minutes at 70ºC. The new synthetized cDNA was stored at -20ºC.

3.5 Reverse Transcriptase Polymerase Chain Reaction (RT-PCR)

The expression of the mRNAs that codify to the enzymes of the polyamine biosynthesis pathway and polyamine receptors was analysed through reverse transcriptase polymerase chain reaction (RT-PCR). This method enables the amplification of a specific portion of DNA sequence. A specific pair of primers were used, each one with complementarity with an extremity of DNA strand. The sequences of the primers used in this work were designed at Primer-BLAST-NCBI-NIH program (NCBI) and are presented in table 3.

For this procedure, KAPPA2G (KAPA Biosystems) Taq DNA polymerase was used to amplify the short DNA fragments, in accordance with manufacturer´s guideline. To each gene test, a MIX was prepared with 5 µL of KAPPA2G Mastermix, 0,3 µL Fw primer, 0,3 µL Rv primer and H_2O sterile up to a final volume of 9,5 µL. Finally, 1 µL of cDNA (1µg) was added to each reaction except for negative control where 1 µL of sterile H_2O was added. To run the PCR protocol, a thermocycler was used. Protocol begun with an initial denaturing time during 3 minutes at 95ºC, followed by 35 cycles of 15 seconds at 95ºC, next 30 seconds at annealing temperature of each primer, 30 seconds at 72ºC and finally 30 seconds at 72ºC.

The PCR products were run on a 1,5% agarose gel with GreenSafe to enable DNA staining. To run the electrophoresis, 3µL of GRS 50 bp Ladder (GRISP) was deposited in the first well and in the other wells 10,5 µL PCR product + 1 µL loading buffer was deposited in each one.

To the full-length fragment, Xpert Taq DNA Polymerase (GRISP) was used in accordance with manufacturer´s recommendation. To each reaction, the MIX was prepared using 5 µL of mastermix, 1µL $MgCl_2$, 0,8 µL Fw primer, 0,8 µL Rv primer and H_20 sterile up to a 9 µL final volume. In the same way as the short fragments, 1 µL of cDNA (1µg) was added to each reaction except for negative control where 1 µL of sterile H_2O was added. PCR protocol was

run at the thermocycler with a denaturing time of 5 minutes at 95ºC followed by 40 cycles of 20 seconds at 95ºC next 30 seconds at optimally annealing temperature and 3 minutes at 72ºC and finally 5 minutes at 72ºC.

PCR products were run on a 1% agarose gel with GreenSafe to enable DNA staining. To run the electrophoresis, 3µL of NZY VIII Ladder (NZYtech) was deposited in the first well and in the other wells 9 µL PCR product + 1 µL loading buffer was deposited in each one.

Table 3 – **Sequences of the primers used in this work**. bp – base pairs. Gapdh is a housekeeping gene and it amplifies at several annealing temperatures; There were no amplification for TAAR2 and TAAR5 at different annealing temperatures.

Gene	Fragment length (bp)		Primer	Annealing temperature (°C)
AMD1	131	Forward	5´-CATCACTCCAGAACCAGAAT-3´	58
		Reverse	5´-TAACAAACAAGGTGGTCACA-3´	
SSAT	101	Forward	5´-GGTTGCAGAAGTGCCGAAAG-3´	60
		Reverse	5´-GTAACTTGCCAATCCACGGG-3´	
Azin1	115	Forward	5´-TGAAGTGCAACTCTGCTCCA-3´	58
		Reverse	5´-TCTGGAGGTACACCCAACTCT-3´	
Oaz1	101	Forward	5´-GAGTTCGCAGAGGAGCAACT-3´	58
		Reverse	5´-CCAAGAAAGCTGAAGGTTCG-3´	
Gapdh	108	Forward	5´- ATGGGGAAGGTGAAGGTCG-3´	-
		Reverse	5´-GGGGTCATTGATGGCAACAATA-3´	
Srm	159	Forward	5´-AAGAACCCGAGCACGAACTT-3´	58
		Reverse	5´-CTGGGCTCAGCTCACATCAT-3´	
Sms	167	Forward	5´-CACAGCACGCTCGACTTCAT-3´	60
		Reverse	5´-AAATTGGCAAAGCTGCCGTT-3´	
ODC1	199	Forward	5´-ACCGGGACAGGATTTGACTG-3´	60
		Reverse	5´-CTTTGGGATGTGCTCTGGCA- 3´	
TAAR1	156	Forward	5´-ACCACACTCGTTGGCAATCT-3´	60
		Reverse	5´-GTGCTCAGCAGATCTCACCA-3´	
TAAR1 (full-length)	1118	Forward	5´-TGATTGACAGCCCTCAGGAAT-3´	58
		Reverse	5´-GTTGGTGCATGTGGTTCGTT-3´	
TAAR2	131	Forward	5´- GGCTGTCTCATCAGAGCAACAT -3´	-
		Reverse	5´- CCACTCGGACACCCAGAGAT -3´	
TAAR5	191	Forward	5´- GGTCATCTACCTGGCCTGTG -3´	-
		Reverse	5´- AGCTCTCCACTGAGCGAATG -3´	

3.5.1 PCR Products Purification

The Wizard® SV Gel and PCR Clean-Up System (Promega) was used to purify PCR products, following the manufacturer's recommendations. Briefly, to a tube containing a PCR product

volume, were added 5 volumes of gel solubilization solution, an agent that denatures the proteins and promotes the link between double strand DNA. Then, the MIX was transferred to a fibrous matrix (column) followed by washing, enabling the elimination of about 99.5% of primers, proteins, salts and other contaminants. Finally, the purified DNA in the column was eluted in a low ionic strength buffer.

3.5.2 PCR Products Cloning in pNZY28 Vector

PCR products were directly cloned using a NZY-A PCR cloning KIT (NZYTech). Since the pNZY28 vector has 3'tymine ends and PCR products have 3'adenosyl ends, the binding of PCR products to the vector is improved and recircularization of the vector is prevented. Moreover, the pNZY28 vector (Figure 9) has a lot of restriction sites, selection regions, a gene that codifies the resistance to ampicillin enabling the selection of bacteria that incorporate the vector, a replication origin (ORI) which enable autonomous replication and transmission to descendance, and finally a multiple cloning region (MCR) that is recognized by multiple restriction enzymes and presents lacZ gene that codifies ß-galactosidase enzyme, which converts x-Gal in a blue compound when vector recircularization occurs and the PCR product is not successfully inserted in the vector. Briefly, to each 3 µL of purified DNA were added 5 µL of NZY-A buffer, 1 µL of pNZY28 vector, and 1 µL of T4 DNA ligase, followed by incubation during 1 hour at room temperature.

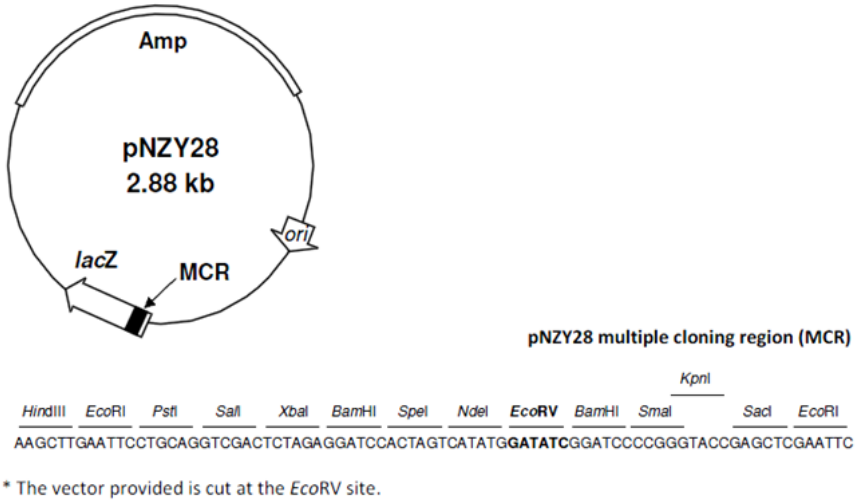

Figure 9 – **pNZY28 cloning vector map** (NZYTech).

3.5.3 *E. coli* Transformation with Recombinant Plasmid

The transformation process of inserting a plasmid into *E. coli* bacteria is only possible if the competent bacteria have the capacity to be transformed with this plasmid. Since this plasmid has a gene that confers resistance to ampicillin, when it is plated in a solid medium containing this antibiotic, only the transformed bacteria can growth and form white colonies. Briefly, 10 µL of the purified PCR product were added to 50 µL of competent cells (frozen at -

80ºC), followed by incubation on ice for 30 minutes and a thermal shock for 1 minute at 42ºC and 2 minutes on ice. The total volume was then seeded in LB/Agar plates containing X-gal (80 µg/mL), isopropyl ß-D-1-thiogalactopyranoside (IPTG) (0.5 mM) and ampicillin (100 µg/mL), and plates were incubated overnight at 37ºC.

3.5.4 Liquid Medium Culture of Recombinant Clones

To obtain a culture with the recombinant clones, a white colony was transferred into a falcon tube containing 2 mL LB-broth medium with ampicillin (100 µg/mL), followed by orbital shaker incubation at 37ºC and 250 rpm for 16 hours.

3.5.5 Recombinant Plasmid Purification

The kit Wizard® Plus SV Minipreps DNA Purification System (Promega) was used to purify the recombinant plasmids, following the manufacturer's protocol. This kit is based in alkaline lysis associated with SDS detergent, enabling the plasmid DNA isolation of *E. coli*, because of their extremely anionic characteristics and larger pH which enable the breakdown of bacterial cell walls and the chromosomal DNA denaturation. A silica column was used to adsorb plasmid DNA by washing the protein and salt impurities. Finally, the plasmid DNA is eluted.

3.5.6 Recombinant Plasmid Digestion

Restriction enzymes recognizes specific nucleotidic sequences in DNA and cut the double chain at a specific location in this sequence. Different bacteria such as *E. coli* synthetizes naturally these enzymes to prevent invasion by viral DNA.

*Eco*R1 enzyme was used for this project and it recognizes the sequence GAATTC hydrolysing G-A phosphodiester link to originate two sticky ends as demonstrated by the following scheme.

5´ G↓AATTC 3´

3´ CTTAA↑G 5´

To 1.5 mL microtubes were added 8 µL of DNA, 2 µL of 10x buffer, 1 µL of the restriction enzyme EcoR1 and 9 µL of sterile H_2O. The samples were incubated during 3 hours at 37ºC. Finally, the enzymatic digestion results were accessed through an 1.5% agarose gel.

3.6 Immunocytochemistry

The immunocytochemistry technique enables protein expression analysis in addition to enable to know their cellular location and distribution.

HIBCPP cells were seemed into 12-wells plates containing a 15 mm diameter coverslip in each well and incubated at 37ºC and 5% CO_2 until they reach around 60-70% confluency.

To prepare the coverslips, they were washed with PBS 1X followed by a 10 minutes fixation time with 4% paraformaldehyde (PFA) at room temperature. After a wash step with PBS 1X, cells were incubated during 1 hour with permeabilization and blocking solution (Triton X-100 0,5% + bovine serum albumin (BSA) 1% in PBS). After washing for five times with phosphate-buffered saline – Tween (PBS-T) 0,01%, the coverslips were incubated overnight with primary antibody (Table 4) previously diluted in antibody dilution solution (BSA 1% in PBS-T 0,01%). Following cells were washed with PBS-T 0,01% and incubated with secondary antibody (Table 4) during an hour in absence of light. After this pass Hoechst 33343 (1:1000, Molecular Probes®) was used to mark the nucleus during 10 minutes at room temperature and in absence of light too.

Finally, blades were mounted using Dako medium and observed in a confocal microscopy LSM 710 (Carl Zeiss) with a 63x objective.

For each experience, two negative controls were performed, a negative-negative control, without primary and secondary antibody to prove that not exist auto fluorescence of the cells and a negative-positive control without primary antibody to verify antibodies specificity.

Table 4 – **Primary and secondary antibodies used to immunocytochemistry**. SPSY (Sms) – spermine synthetase; ODC1 – ornithine decarboxylase 1.

Protein	Primary antibody	Dilution	Company	Secondary antibody	Dilution	Company
SPSY (Sms)	Polyclonal rabbit anti-SPSY (sc-99159)	1:50	Santa Cruz Biotechnology, Inc	Alexa Fluor 488 anti-Rabbit	1:1000	Molecular Probes®
ODC1	Monoclonal mouse anti-ODC1 (sc-398116)	1:25	Santa Cruz Biotechnology, Inc	Alexa Fluor 488 anti-Mouse	1:1000	Molecular Probes®

3.7 Western Blot

Western blot technique enables the analysis of protein expression in different tissues or cells.

To total protein extraction, HIBCPP cells were recovered and washed with PBS 1X, followed by a 7 minutes centrifugation time at 11000 g and 4ºC with collection of the supernatant. Finally, cells were resuspended in lysis buffer RIPA (5 mM HEPES (pH 7,5), 250 mM sucrose, 10 mM $NaNO_3$, 0,2 mM phenylmethylsulphonyl fluoride (PMSF), 25 µg/mL Leupeptin, 1 mM orthovanadate, 10 mM sodium phosphate (pH 7,4), 150 mM NaCl, 2% Triton X-100, 2% deoxycholate, 0,2% sodium dodecyl sulphate (SDS) and 0,2 mM PMSF). Protein content in the samples was quantified using Pierce™ BCA Protein Assay Kit (ThermoFischer) according to the manufacturer´s guidelines.

A polyacrylamide gel composed by two different gels, the resolving (12,5%) and the stacking (4,7%) was prepared. Ammonium persulfate (PSA) 10% and TEMED (catalyser) were added to resolving gel and it was deposed between the glasses followed by the addiction of the same reagents to stacking gel and their deposition above the previous, with an immediate placement of the respective combs.

Samples were prepared with 40 µg of protein and loading buffer (Glycerol, 10% SDS, Tris-HCl 1.5M, bromophenol blue, 4% ß-mercaptoethanol) followed by a denaturation step of 10 minutes at 95ºC and deposition in the gel wells.

After electrophoresis, the electro transference pass started and the deposition gel was equilibrated during 10 minutes in electro transference buffer as the PVDF 0,45 µm membrane previously activated in pure methanol. Sandwich was mounted with the following order: four filter papers, membrane, gel and four filter papers newly, and this mount was placed in Bio-Rad Turbo (Bio-Rad) for 30 minutes and 25V. When transference was completed, membrane was washed in TBS 1X (Tris-buffered saline) and placed in blocking solution (5% light milk in 0,01% TBS-T) for 1 hour at room temperature. In the next step membranes were incubated overnight at 4ºC with primary antibody (Table 5). In the following day 3 washes with TBS-T 0,01% were preformed and membranes were incubated for 1 hour at room temperature with the secondary antibody (Table 5). Before reveal, membranes were washed two times in TBS-T 0,01% and next they were revealed using ECL (Milippore) in the ChemiDoc system (Bio-Rad).

Table 5 – **Primary and secondary antibodies used to Western blot.** SPSY (Sms) – spermine synthetase; ODC1 – ornithine decarboxylase 1.

Protein	Primary antibody	Dilution	Company	Secondary antibody	Dilution	Company
SPSY (Sms)	Polyclonal rabbit anti-SPSY (sc-99159)	1:100	Santa Cruz Biotechnology, Inc	anti-Rabbit	1:40000	Santa Cruz Biotechnology, Inc
ODC1	Monoclonal mouse anti-ODC1 (sc-398116)	1:75	Santa Cruz Biotechnology, Inc	anti-Mouse	1:40000	Santa Cruz Biotechnology, Inc

3.8 MTT Assay

A MTT assay was preformed to ensure that the cadaverine stimuli did not impair HIBCPP cells viability. Briefly, about 15000 cells were seeded per well in 96-multiwell plates and incubated at 37ºC and 5% CO2 until reach 60-70% cellular confluence. The different stimuli were then applied to HIBCPP cells, as shown in figure 10. After 12h and 24h of incubation time, the MTT solution was added, followed by 3 hours incubation, avoiding light exposure. DMSO solution was added to solve formazan crystals and the plate was placed in an agitator for 30 minutes, followed by 570 nm absorbance read.

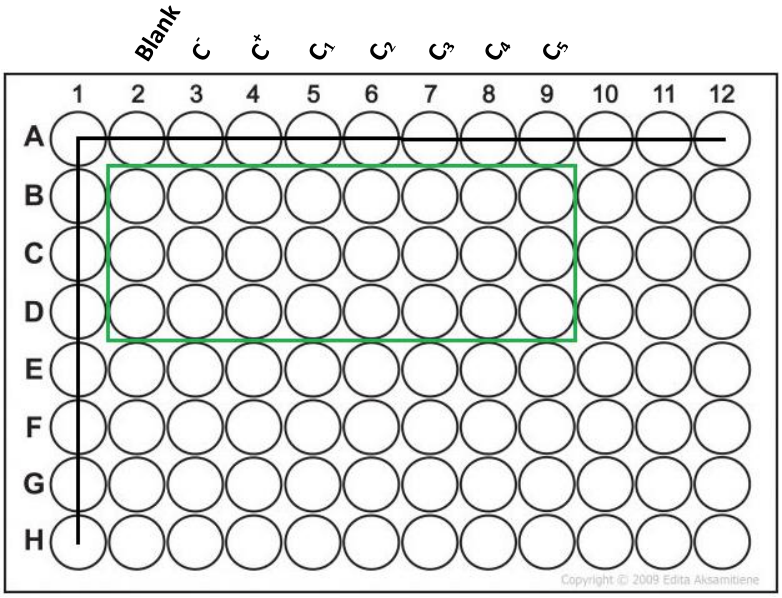

Figure 10 – **Representative scheme of the MTT assay.** Blank – only complete DMEM/F12 culture medium; C^- - Cells with complete DMEM/F12 culture medium; C^+ - Cells with complete DMEM/F12 culture medium + 70% ethanol; C_1-C_5 – Cells with complete DMEM/F12 culture medium + cadaverine stimulus in different concentrations.

3.9 Calcium Imaging

The Ca^{2+} imaging enables the detection of intracellular calcium changes in response to a stimulus. The fluorescent molecule Fura-2AM (Molecular Probes®) was used in this work. At a free state without Ca^{2+}, this probe has larger fluorescence at 380 nm than 340 nm while when it was linked to Ca^{2+}, 380 nm fluorescence decrease and 340 nm fluorescence rises. HIBCPP cells were seeded in 8 µ-slide plates (Ibidi) and grown until reach a 70-80% confluence. Cells were then washed twice with complete DMEM/F12 and incubated during an hour with Fura-2AM (5µM) probe diluted in complete DMEM/F12 + 0,02% pluronic acid (Pluronic® F-127, Invitrogen), followed by incubation for 30 minutes with Tyrode´s solution, a roughly isotonic with interstitial fluid solution, composed by NaCl 140 mM, KCl 5 mM, $MgCl_2$ 1 mM, $CaCl_2$ 2 mM, napyruvate 10 mM, glucose 10 mM, Hepes 10 mM, and $NaHCO_3$ 5 mM, with a final pH of 7.4. Finally, cells were observed under an Axio Imager A1 microscope (Zeiss) and different polyamines stimuli were added and Ca^{2+} changes were measured through fluorescence ratio emitted at 520nm after 340 nm and 380 nm excitation, using as light source Lambda DG4 (Sutter Instruments) with a 40x objective and a AxioVision (Carl Zeiss) camera. The AxioVision (Carl Zeiss) software enabled image acquisition.

To test the HIBCPP cells response, cadaverine in different concentrations were applied as shown by table 6.

Data were processed using Fiji software (MediaWiki).

Table 6 – **Cadaverine concentrations applied to HIBCPP cells.**

Compound	Concentrations				
Cadaverine	2 mM	1 mM	500 µM	250 µM	125 µM

3.10 Cells Transfection

To analyse the TAAR1 activation specificity, HIBCPP cells were transfected with a Silencer® Select siRNAs (Ambion, ThermoFischer) for TAAR1. Around 50.000 cells were seeded in 8 µ-slide plates (Ibidi) and grown until reach a confluence around 60%. 24 hours before starts the transfection process the complete DMEM/F12 medium was changed to DMEM/F12 medium without antibiotic.

Transfection MIX was prepared with Opti-MEM (Invitrogen) culture medium with a concentration of 10 nM of TAAR1 small interfering RNA (siRNA) and 5 nM of Lipofectamine 2000 (ThermoFisher). A control for TAAR1 siRNA specificity was prepared with 10 nM of

scramble siRNA (4390843, ThermoFisher) and 5 nM of Lipofectamine too. As other control for this assay, cells were incubated only with 5 nM of Lipofectamine.

Cells were incubated during 72 hours at 37ºC and 5% CO_2, after which Ca^{2+} imaging was performed to analyse the receptor silencing.

3.11 Statistical Analysis

Statistical analysis of calcium imaging and MTT assays in HIBCPP cells were performed with GraphPad Prism (Version 6). Data were compared and expressed as mean ± SEM. The comparisons made between the means of two different groups were performed using one and two-way ANOVA followed by Bonferroni´s test. Results were considered statistical significant when $p < 0.05$.

Chapter 4

4. Results

4. Results

4.1 Data Base Search

A search done using BlastX (NCBI) tool enabled to quantify the percentage of homology between the human TAAR genes and the zebrafish TAAR13c.

A comparison with the Gene Expression Omnibus data base enabled to confirm that TAAR1, 2 and 5 were the most abundant TAARs in humans among those that were identified with higher homology with TAAR13c.

Table 7 shows the TAAR1, 2 and 5 homologies to TAAR13c.

Table 7 – **Homology between human TAAR genes and zebrafish TAAR13c.** Homology percent obtained with BlastX (NCBI) search.

Human TAAR gene	Homology with zebrafish TAAR13c
TAAR1	45%
TAAR2	45%
TAAR5	43%

4.2 Expression Analysis of TAAR1, 2 and 5 in Human CP

4.2.1 Genic Expression of TAAR1 (RT-PCR)

RT-PCR revealed the expression of TAAR1 mRNA in HIBCPP cells trough specific amplification of nucleotides sequences of TAAR1 gene. A 1,5% agarose gel stained with GreenSafe was preformed to run the amplified product and, comparing with GRS 50 bp Ladder (GRISP) (M), the obtained size of TAAR1 fragment gene was ~156 bp (figure 11).

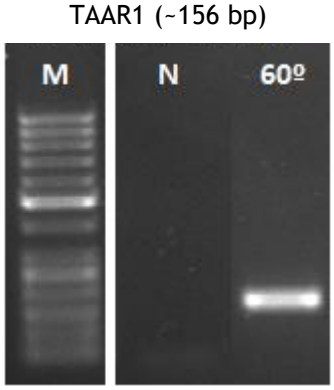

Figure 11 - **Electrophoresis in 1.5% agarose gel stained with GreenSafe of cDNA PCR products of TAAR1 gene.** M- NZY VIII Ladder marker; N- negative control without cDNA.

Another RT-PCR was done for the full-length TAAR1 but, in this case, a 1% agarose gel stained with GreenSafe (NZYTech) was used and NZY VIII Ladder (M) used as length marker. The size of the obtained fragment corresponds to the expected ~1118 bp (figure 12). No amplification was verified in the negative controls (N), which prove the absence of contamination.

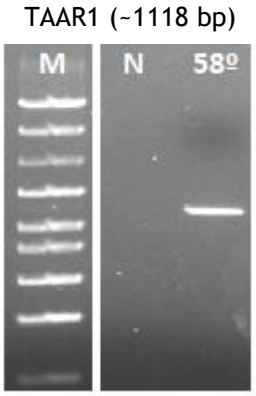

Figure 12 - **Electrophoresis in 1% agarose gel stained with GreenSafe of cDNA PCR products of TAAR1 full-length gene.** M- NZY VIII Ladder marker; N- negative control without cDNA.

These PCR products were purified and cloned in pNZY28 vector before sent to Sanger Sequencing to "Stabvida Portugal" company. Resulting sequences were aligned with human genome in NCBI-BLAST (http://blast.ncbi.nlm.nih.gov/) presenting 100% homology. With these results, the expression at mRNA level of TAAR1 gene was demonstrated in human CP (table 8).

Table 8 – **Resume of the homologies of TAAR1 with human cDNA data base.**

Gene	Homology with human cDNA data base
TAAR1 (short-fragment)	100%
TAAR1 (full-length)	100%

4.2.2 Gene Expression of TAAR2 and TAAR5 (RT-PCR)

After different optimization steps of the RT-PCR protocol, there were no amplification to the TAAR2 and TAAR5 fragments in the HIBCPP cell line.

4.3 Polyamines Biosynthetic Pathway

4.3.1 Polyamines Biosynthetic Pathway Genic Analysis by RT-PCR in Human CP Cell Line

RT-PCR results confirm the expression of ODC1, Srm, and Sms mRNAs in HIBCPP cells, trough specific amplification. A 1,5% agarose gel stained with GreenSafe was used to separate the amplified products and, comparing with 50 bp GRS Ladder (GRISP) (M), the size of the obtained fragments corresponds to the expected, 199 bp (figure 13A), 159 bp (figure 13B) and 167 bp (figure 13C), respectively. No amplification was observed in the negative controls (N).

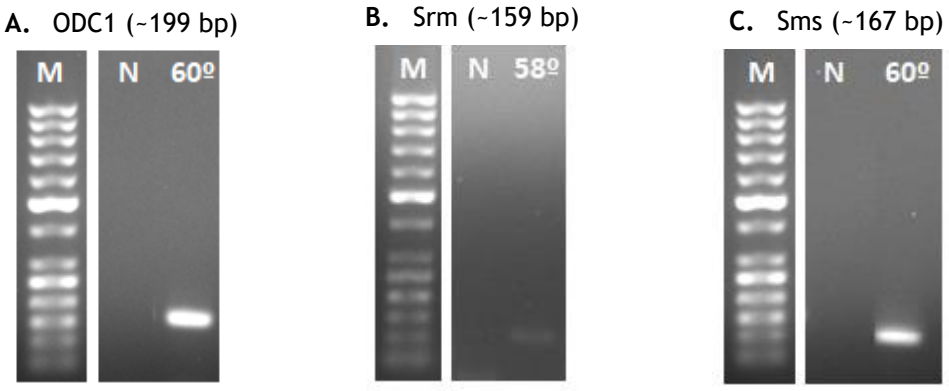

Figure 13 - **Electrophoresis in 1.5% agarose gel stained with GreenSafe of cDNA PCR products of polyamines pathway enzymes genes.** A- ODC1 (~199 bp); B- Srm (~159 bp); C- Sms (~167 bp); N- negative control without cDNA.

PCR products were Sanger sequenced (at "Stabvida Portugal") and the resulting sequences were aligned with the human cDNA data base in NCBI-BLAST (http://blast.ncbi.nlm.nih.gov/) presenting homology percentages up to 98%. With these results, the presence of mRNA transcripts for ODC1, Srm and Sms genes were demonstrated in human CP cell line (table 9).

Table 9 – **Genes for polyamines biosynthetic pathway enzymes identified in human CP.**

Gene	Homology with cDNA data base
ODC1	99%
Srm	98%
Sms	100%

4.3.2 Protein Expression Analysis of Biosynthetic Pathway of Polyamines (Western Blot)

Spermine synthase, SPSY (Sms) protein was detected in HIBCPP cell protein extracts by Western blot corresponding to a band of approximately 43 kDa. In this blot it was possible to see some unspecific bands which probably correspond to other isoforms of this protein (Figure 14).

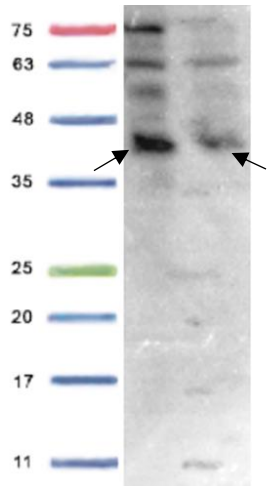

Figure 14 – **Western blot of total protein extracts of HIBCPP cells with SPSY (Sms) antibody.**

Ornithine decarboxylase (ODC1) protein was detected in cell protein extracts by Western blot corresponding to a band of approximability 48 kDa (Figure 15).

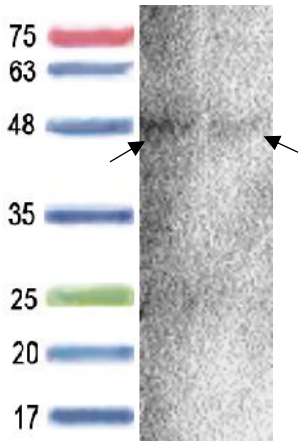

Figure 15 – **Western blot of total protein extracts of HIBCPP cells with ODC1 antibody.**

4.3.3 Protein Expression Analysis of Biosynthetic Pathway of Polyamines (Immunocytochemistry)

The results of the immunocytochemistry visualization with specific SPSY (Sms) (Figure 16) and ODC1 (Figure 17) antibodies enabled cytoplasmic detection of the SPSY (Sms) and ODC1 protein in HIBCPP cells. There was no staining in the negative controls.

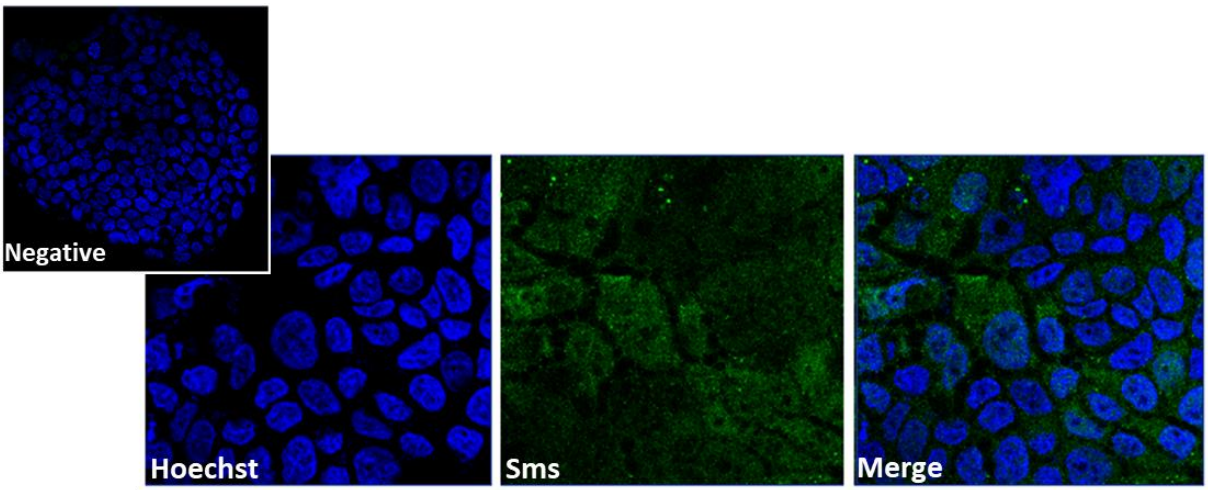

Figure 16 - **Expression and localization of Spermine synthase, SPSY (Sms) in HIBCPP cells by confocal microscopy.** Magnification: 63x. There was no staining in the negative control.

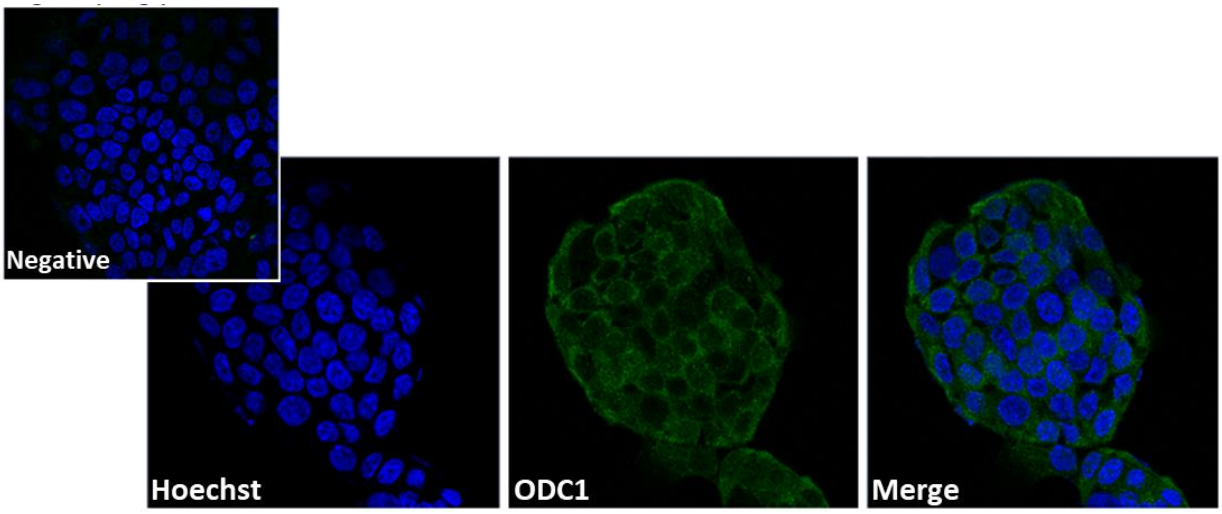

Figure 17 - **Expression and localization of Ornithine decarboxylase 1 (ODC1) in HIBCPP cells by confocal microscopy.** Magnification: 63x. There was no staining in the negative control.

4.4 Polyamines Catabolic Pathway

4.4.1 Polyamines Catabolic Pathway Genic Analysis by RT-PCR in Human CP Cell Line

RT-PCR also enabled the detection of Azin1, AMD1, SSAT, and Oaz1 mRNAs in HIBCPP cells. A 1,5% agarose gel stained with GreenSafe was run with the amplified products and, comparing with 50 bp GRS Ladder (GRISP) (M), the size of the obtained fragments was the expected: 115 bp (figure 18A), 131 bp (figure 18B), 101 bp (figure 18C) and 101 bp (figure 18D), respectively. No amplification was observed in the negative controls (N), without cDNA.

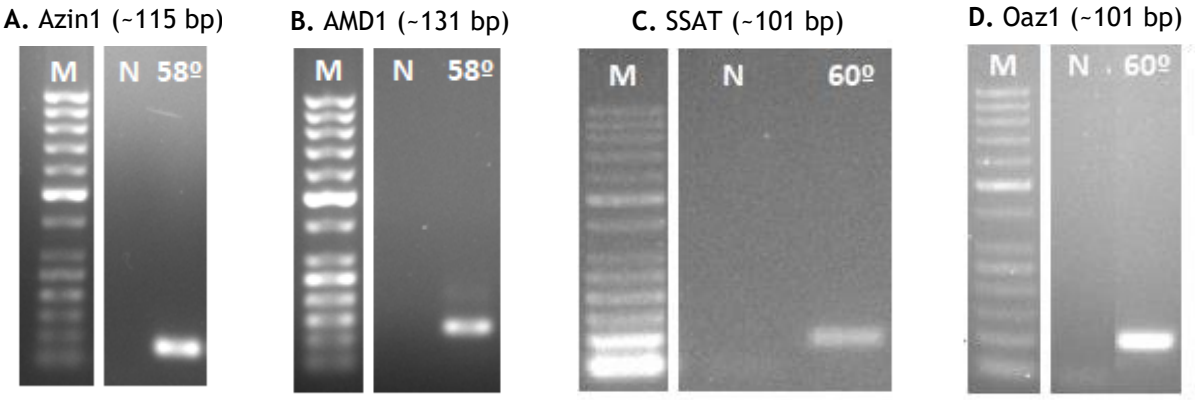

Figure 18 - **Electrophoresis in 1.5% agarose gel stained with GreenSafe of cDNA PCR products of polyamines catabolic pathway genes.** A- Azin1 (~115 bp); B- AMD1 (~131 bp); C- SSAT (~101 bp); D- Oaz1 (~101 bp). There was no amplification in the negative controls without cDNA (N).

PCR products were Sanger sequenced (at "Stabvida Portugal") and the resulting sequences were aligned with the human cDNA data base in NCBI-BLAST (http://blast.ncbi.nlm.nih.gov/) presenting homology percentages up to 96%. With these results, the expression at mRNA level of Azin1, AMD1, SSAT and Oaz1 genes were demonstrated in the human CP cell line (table 10).

Table 10 – **Genes for polyamines catabolic pathway enzymes identified in human CP cell line.**

Gene	Homology with human cDNA data base
Azin1	97%
AMD1	97%
SSAT	96%
Oaz1	98%

4.5 Cellular Viability (MTT)

HIBCPP cell viability was analysed, using the MTT assay, for all cadaverine concentrations used in our study. The assays were performed for two different incubation times, 12 and 24 hours. It was possible to see a reduction in cell viability to 2 mM concentration but after statistical analysis the results had not significance when compared with the negative control. There was significative differences between the negative and positive controls as expected. Data are shown in figure 19.

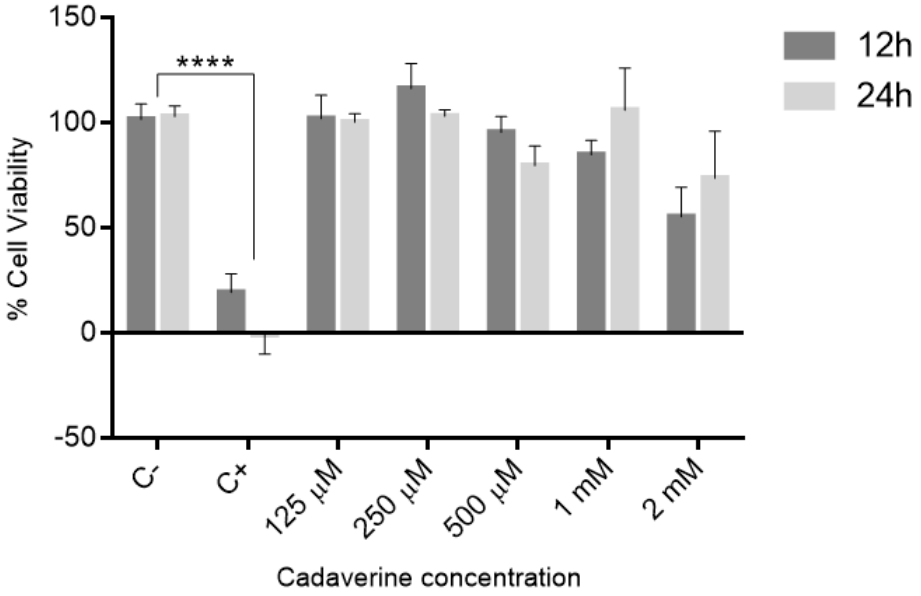

Figure 19 – **Graphical representation of the cellular viabilities with cadaverine incubation for 12 and 24 hours.** Data were compared and expressed as mean ± SEM. Statistical analysis was performed using two-way ANOVA followed by Bonferroni's multiple comparisons test. **** refers to significance which exists between the controls (negative and positive) (p< 0.0001). Results were considered statistical significant when p <0.05.

4.6 Calcium Imaging

To analyse the "olfactory response" of the HIBCPP cells to the polyamines stimulus, the single cell Ca^{2+} imaging technique was performed using increasing concentrations of cadaverine.

The results obtained from increasing concentrations of cadaverine (125, 250, 500 and 1000µM) are presented in figure 20, with a dose-related response. The statistical analysis revealed differences between 125 and 500 µM and between 125, 250 and 500 µM and 1 mM.

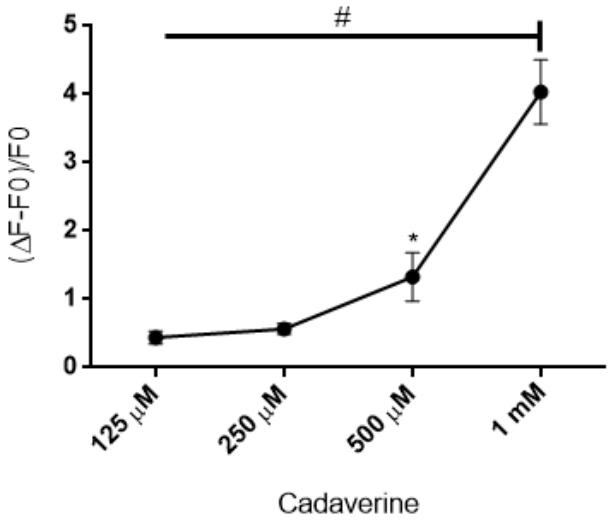

Figure 20 – **Representation of the HIBCPP Ca^{2+} cells response with cadaverine stimuli.** ΔF represents the reason between F_{380} and F_{340} (F_{380}/F_{340}); F0 represents the fluorescence baseline. Data were compared and expressed as mean ± SEM. * refers to significance which exists between 125 µM and 500 µM stimulus (*p* 0.0406); # refers to significance which exists between 125, 250 and 500 µM and 1 mM stimulus (*p*< 0.0001). Statistical analysis was performed using one-way ANOVA followed by Bonferroni's multiple comparisons test. Results were considered statistical significant when *p* <0.05.

4.7 Cells Transfection

To analyse if TAAR1 was responsible for the HIBCPP cells response to cadaverine, cells were transfected with TAAR1 siRNA or scramble siRNA and their responses to cadaverine stimuli were measured by Ca^{2+} imaging.

As seen in figure 21, a preliminary assay (n=1) with duplicates, revealed a reduction in transfected cells response to cadaverine when compared with the control groups (Lipofectamine or Lipofectamine + scramble siRNA).

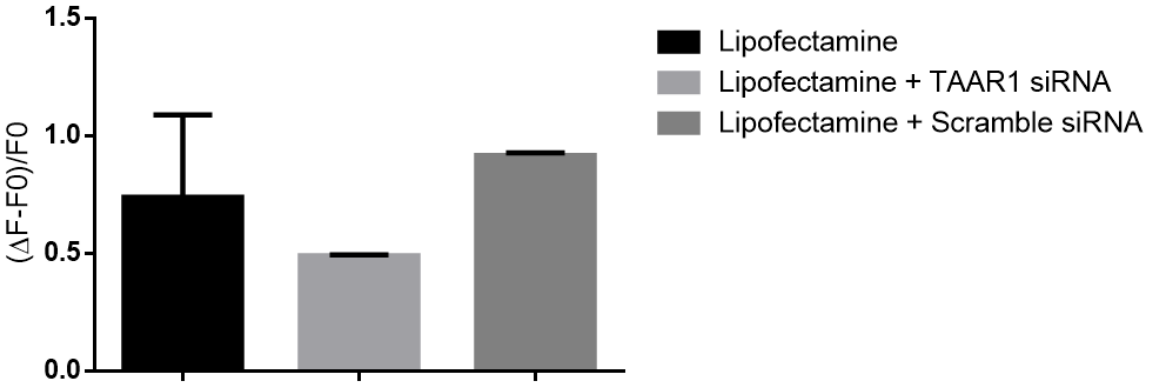

Figure 21 –**Ca^{2+} responses of HIBCPP cells response to cadaverine were inhibited after TAAR1 silencing with 10nM of siRNA.** ΔF represents the reason between F_{380} and F_{340} (F_{380}/F_{340}); F0 represents the fluorescence baseline. Fluorescence ratio chance $\Delta F(F_{380}/F_{340})$, loaded with Fura-2AM and stimulated with 1 mM of cadaverine. Data are presented as the mean ± SEM. No statistical analysis was done because n=1.

Chapter 5

5. Discussion

5. Discussion

The choroid plexus is a highly vascularized structure localized in the brain ventricular spaces with an important function in the surveillance of blood and CSF composition maintaining the brain homeostasis. Several different mechanisms are involved in this process, but these are not fully clarified yet. Previous studies by our group disclosed to additional pathways that might be fundamental players in chemo surveillance; the taste and odorant pathways, which seem to be functional in the CP epithelia (Quintela et al. 2013; Gonçalves et al. 2016). Gonçalves *et al*. 2016 proved that CP explants can produce electrophysiological responses when stimulated with different polyamines: cadaverine, spermine, spermidine and putrescine (Gonçalves et al. 2016).

A polyamine like cadaverine is a polycation which appear naturally in cells through lysine decarboxylation (Tabor & Tabor 1985; Tomar et al. 2013). On the other hand, cadaverine can be produced by the decaying of tissues. In the zebrafish, for example, cadaverine is dissolved in the sea water and later it can be detected by the TAAR13c expressed in the olfactory epithelium of this fish species (Hussain et al. 2013). This mechanism leads to aversion of rotten animals.

A preliminary research using BlastX and the National Centre for Biotechnology Information data base allowed to identify the human TAARs with the highest homology to zebrafish TAAR13c. After some TAARs have been identified as the receptors with the highest homology, a comparison with cDNA microarrays results enabled to choose TAAR1, TAAR2 and TAAR5 as the target receptors for this project due to its higher level of expression in human CP tissues (Gene Expression Omnibus data base) (Janssen et al. 2013).

Thus, we started to confirm the expression of TAAR1, TAAR2 and TAAR5 mRNA by the RT-PCR technique. There was no amplification for TAAR2 and TAAR5, so we stayed focused in TAAR1. Initially a fragment of 156 bp was amplified from CP cDNA that was 100% homologous to TAAR1. Next the full-length fragment of TAAR1 gene (1118 bp) was amplified from CP cDNA and cloned in pNZY28 with 100% homology with the reference sequence of NCBI human cDNA data base.

After the confirmation of TAAR1 mRNA expression in the CP, we analysed the expression of the mRNAs that encode enzymes of the biosynthetic pathway of polyamines using RT-PCR. The expression of ODC1, Srm and Sms were demonstrated in human CP cells, sharing up to 98% homology with the NCBI human cDNA data base.

Western blot technique enabled SPSY (Sms) and ODC1 protein detection in protein extracts from CP cells. A specific SPSY antibody detected a band with 43 kDa of molecular weight as

described in the literature (Korhonen et al. 2001). An ODC1 antibody detected a band with around 48 kDa of molecular weight unlike the 51 kDa described in the literature (Tian et al. 2006).

SPSY (Sms) and ODC1 proteins were also localized in HIBCPP cells by immunocytochemistry. Specific SPSY and ODC1 antibodies detected Sms protein presence in CP cells with greater expression at the cytoplasmic level as described by Kang *et al*. and ODC1 protein showed too cytoplasmic expression as described by Schipper *et al*. (Schipper & Verhofstad 2002; Schipper et al. 2004; Kang et al. 2018).

In a following step, the expression of the genes encoding the enzymes involved in the polyamines' catabolic pathway, Azin1, AMD1, SSAT and Oaz1 were confirmed by RT-PCR followed by Sanger sequencing with homology up to 96% when compared with NCBI gene bank.

With the confirmation of the expression of a trace amines receptor (TAAR1), the biosynthesis pathway of polyamine´s enzymes and of catabolic pathway of polyamines in CP, it was time to carry out Ca^{2+} imaging assays with cadaverine stimulus. Beforehand, however, the effects of this polyamine in cellular viability were tested by the MTT assay.

The MTT assay enabled to prove that the different concentrations of cadaverine applied to CP cells (125 µM, 250 µM, 500 µM, 1 mM and 2 mM) did not compromise their viability.

Then, we perform the Ca^{2+} imaging technique to measure the intracellular concentrations of Ca^{2+} after stimulation with cadaverine. The results obtained show that cells respond to concentrations of up to 125 µM with a very expressive response for 1 mM of cadaverine.

Aiming at analysing the specificity of TAAR1 activation by cadaverine, we proceeded to the siRNA transfection assays to silence TAAR1.

Preliminary results revealed a notable reduction of the Ca^{2+} responses to cadaverine in the TAAR1 siRNA transfected HIBCPP cells. This reduction was observed when responses were compared with the controls (lipofectamine or lipofectamine + scramble siRNA).

Based on the results of the present work, which have bridged the previous studies in rats and the human choroid plexus, we can say for the first time that the gene coding for TAAR1 is expressed in the human CP cells as well as all the genes for the enzymes of the biosynthetic and catabolic pathways of the polyamines.

The results of this work enable to confirm the strong response of the CP cells to cadaverine stimulus leading to an increase in intracellular levels of Ca^{2+}, which was decreased when cells were transfected with TAAR1 siRNA.

Chapter 6

6. Conclusion and Future Perspectives

6. Conclusion and Future Perspectives

With this work it was possible to prove that TAAR1 mRNA is expressed in the human CP cells as well as all the genes encoding the enzymes of the biosynthetic and catabolic pathways of the polyamines.

It was showed too that the HIBCPP cells present a dose-related response when stimulated with increasing concentrations of cadaverine.

Finally, with a premature analysis of the results we can predict that the TAAR1 is probably the receptor that binds cadaverine triggering a Ca^{2+} response in CP cells.

Once the TAAR1 mRNA expression has been demonstrated in HIBCPP cells, it would be interesting to demonstrate both the expression of its protein by Western blot as well as its cellular location by immunocytochemistry. It would also be important to perform Ca^{2+} imaging tests using other polyamines such as spermine, spermidine and putrescine to verify if TAAR1 is also involved in their detection. Silencing assays, using transfected cells with TAAR1 siRNA will enable to prove if TAAR1 is the receptor responsible for detecting other polyamines as spermine, spermidine and putrescine.

Chapter 7

7. References

7. References

Abbott, N.J. et al., 2010. Structure and function of the blood-brain barrier. *Neurobiology of Disease*, 37(1), pp.13–25.

Antony, T. et al., 2003. Cellular polyamines promote the aggregation of alpha-synuclein. *Journal of Biological Chemistry*, 278(5), pp.3235–3240.

Asif-Malik, A., Hoener, M.C. & Canales, J.J., 2017. Interaction between the Trace Amine-Associated Receptor 1 and the Dopamine D2 Receptor Controls Cocaine's Neurochemical Actions. *Scientific Reports*, 7(1), pp.1–12.

Bachrach, U., Wang, Y.C. & Tabib, A., 2001. Polyamines: new cues in cellular signal transduction. *News in physiological sciences*, 16(June), pp.106–9.

Balusu, S. et al., 2016. The choroid plexus-cerebrospinal fluid interface in Alzheimers disease: More than just a barrier. *Neural Regeneration Research*, 11(4), pp.534–537.

Bell, M.R. et al., 2011. A neuroprotective role for polyamines in a Xenopus tadpole model of epilepsy. *Nature Neuroscience*, 14(4), pp.505–512.

Bernd, A. et al., 2015. Characterization of efflux transport proteins of the human choroid plexus papilloma cell line HIBCPP, a functional in vitro model of the blood-cerebrospinal fluid barrier. *Pharmaceutical Research*, 32(9), pp.2973–2982.

Berry, M.D., 2004. Mammalian central nervous system trace amines. Pharmacologic amphetamines, physiologic neuromodulators. *Journal of Neurochemistry*, 90(2), pp.257–271.

Berry, M.D. et al., 2017. Pharmacology of human trace amine-associated receptors: Therapeutic opportunities and challenges. *Pharmacology and Therapeutics*, 180, pp.161–180.

Borowsky, B. et al., 2001. Trace amines: Identification of a family of mammalian G protein-coupled receptors. *Proceedings of the National Academy of Sciences*, 98(16), pp.8966–8971.

Bradaia, A. et al., 2009. The selective antagonist EPPTB reveals TAAR1-mediated regulatory mechanisms in dopaminergic neurons of the mesolimbic system. *Proceedings of the National Academy of Sciences*, 106(47), pp.20081–20086.

Branchek, T.A. & Blackburn, T.P., 2003. Trace amine receptors as targets for novel therapeutics: Legend, myth and fact. *Current Opinion in Pharmacology*, 3(1), pp.90–97.

Brinker, T. et al., 2014. A new look at cerebrospinal fluid circulation. *Fluids and Barriers of the CNS*, 11(1), p.10.

Bruch, R.C., 1996. Phosphoinositide second messengers in olfaction. *Comparative Biochemistry and Physiology B Biochemistry Molecular Biology*, 113(3), pp.451–459.

Buck, L. & Axel, R., 1991. A novel multigene family may encode odorant receptors: a molecular basis for odor recognition. *Cell*, 65(1), pp.175–187.

Bunzow et al., 2001. Amphetamine, 3,4-methylenedioxymethamphetamine, lysergic acid diethylamide, and metabolites of the catecholamine neurotransmitters are agonists of a rat trace amine receptor. *Molecular Pharmacology*, 60(6), pp.1181–1188.

Burchett, S.A. & Hicks, T.P., 2006. The mysterious trace amines: Protean neuromodulators of synaptic transmission in mammalian brain. *Progress in Neurobiology*, 79(5–6), pp.223–246.

Campilongo, R. et al., 2014. Molecular and functional profiling of the polyamine content in enteroinvasive E. coli: Looking into the gap between commensal E. coli and harmful Shigella. *PLoS ONE*, 9(9).

Chandrashekar, J. et al., 2006. The receptors and cells for mammalian taste. *Nature*, 444(7117), pp.288–294.

Chaudhari, N. & Roper, S.D., 2010. The cell biology of taste. *Journal of Cell Biology*, 190(3), pp.285–296.

Chiellini, G. et al., 2012. Distribution of exogenous [125I]-3-iodothyronamine in mouse in vivo: Relationship with trace amine-associated receptors. *Journal of Endocrinology*, 213(3), pp.223–230.

Chiellini, G. et al., 2007. Cardiac effects of 3-iodothyronamine: A new aminergic systemmodulat- ing cardiac function. *FASEB Journal*, 21, pp.1597–1608.

Choudhuri, S. et al., 2003. Constitutive expression of various xenobiotic and endobiotic transporter mRNAs in the choroid plexus of rats. *Drug Metabolism and Disposition*, 31(11), pp.1337–1345.

Clark, A.A. et al., 2015. TAS2R bitter taste receptors regulate thyroid function. *The FASEB Journal*, 29(1), pp.164–172.

Cöster, M. et al., 2015. Evolutionary Conservation of 3-Iodothyronamine as an Agonist at the Trace Amine-Associated Receptor 1. *European Thyroid Journal*, 4(Suppl 1), pp.9–20.

D´Andrea, G. et al., 2003. HPLC electrochemical detection of trace amines in human plasma and platelets and expression of mRNA transcripts of trace amine receptors in circulating leukocytes. *Neuroscience Letters*, 346(1–2), pp.89–92.

Damkier, H.H., Brown, P.D. & Praetorius, J., 2013. Cerebrospinal Fluid Secretion by the Choroid Plexus. *Physiological Reviews*, 93(4), pp.1847–1892.

Danielski, L.G. et al., 2017. Brain Barrier Breakdown as a Cause and Consequence of Neuroinflammation in Sepsis. *Molecular Neurobiology*, 55(2), pp.1–9.

Depoortere, I., 2014. Taste receptors of the gut: emerging roles in health and disease. *Gut*, 63(1), pp.179–90.

Dewan, A. et al., 2013. Non-redundant coding of aversive odours in the main olfactory pathway. *Nature*, 497(7450), pp.486–489.

Dieris, M. et al., 2017. A single identified glomerulus in the zebrafish olfactory bulb carries the high-affinity response to death-associated odor cadaverine. *Scientific Reports*, 7(January), p.40892.

Dinter, J., Mühlhaus, J., Jacobi, S.F., et al., 2015. 3-iodothyronamine differentially modulates α-2A-adrenergic receptor-mediated signaling. *Journal of Molecular Endocrinology*, 54(3), pp.205–216.

Dinter, J., Mühlhaus, J., Wienchol, C.L., et al., 2015. Inverse agonistic action of 3-iodothyronamine at the human trace amine-associated receptor 5. *PLoS ONE*, 10(2), pp.1–19.

Du, L. et al., 2013. Recent advances in olfactory receptor-based biosensors. *Biosensors and Bioelectronics*, 42(1), pp.570–580.

Duan, Bo; Wang, Yi-Zhi; Yang, T. et al., 2011. Extracellular Spermine Exacerbates Ischemic Neuronal Injury through Sensitization of ASIC1a Channels to Extracellular Acidosis. *Journal of Neuroscience*, 31(6), pp.2101–2112.

Duan, J. et al., 2004. Polymorphisms in the Trace Amine Receptor 4 (TRAR4) Gene on Chromosome 6q23.2 Are Associated with Susceptibility to Schizophrenia. *The American Journal of Human Genetics*, 75(4), pp.624–638.

Duarte, A.C. et al., 2016. Sex Hormone Decline and Amyloid ß Synthesis, Transport and Clearance in the Brain. *Journal of Neuroendocrinology*, 28(11).

Ek, C.J. et al., 2010. Efflux mechanisms at the developing brain barriers: ABC-transporters in the fetal and postnatal rat. *Toxicology Letters*, 197(1), pp.51–59.

Ekegren, T. & Gomes-Trolin, C., 2005. Determination of polyamines in human tissues by precolumn derivatization with 9-fluorenylmethyl chloroformate and high-performance liquid chromatography. *Analytical Biochemistry*, 338(2), pp.179–185.

Espinoza, S. et al., 2015. TAAR1 Modulates Cortical Glutamate NMDA Receptor Function. *Neuropsychopharmacology*, 40(9), pp.2217–2227.

Falcão, Ana Mendanha; Marques, Fernanda, Novais, Ashley; Sousa, Nuno; Palha, Joana Almeida; Sousa, J.C., 2012. The path from the choroid plexus to the subventricular zone: go with the flow! *Frontiers in Cellular Neuroscience*, 6((August)), pp.1–8.

Ferrero, D.M. et al., 2012. Agonists for 13 trace amine-associated receptors provide insight into the molecular basis of odor selectivity. *ACS Chemical Biology*, 7(7), pp.1184–1189.

Ferrero, D.M. et al., 2011. Detection and avoidance of a carnivore odor by prey. *Proceedings of the National Academy of Sciences*, 108(27), pp.11235–11240.

Gevrekci, A.Ö., 2017. The roles of polyamines in microorganisms. *World Journal of Microbiology and Biotechnology*, 33(11), p.204.

Ghersi-Egea, J.F. et al., 2009. Blood-brain interfaces and cerebral drug bioavailability. *Revue Neurologique*, 165(12), pp.1029–1038.

Ghersi-Egea, J.F. et al., 2006. Brain protection at the blood-cerebrospinal fluid interface involves a glutathione-dependent metabolic barrier mechanism. *Journal of Cerebral Blood Flow and Metabolism*, 26(9), pp.1165–1175.

Ghersi-Egea, J.F. et al., 1994. Localization of Drug-Metabolizing Enzyme Activities to Blood-Brain Interfaces and Circumventricular Organs. *Journal of Neurochemistry*, 62(3), pp.1089–1096.

Gloriam, D.E.I. et al., 2005. The repertoire of trace amine G-protein-coupled receptors: Large expansion in zebrafish. *Molecular Phylogenetics and Evolution*, 35(2), pp.470–482.

Gomes-Trolin, C. et al., 2002. Increased red blood cell polyamines in ALS and Parkinson's disease. *Experimental Neurology*, 177(2), pp.515–520.

Gonçalves, I. et al., 2016. Smelling the cerebrospinal fluid: Olfactory signaling molecules are expressed in and mediate chemosensory signaling from the choroid plexus. *FEBS Journal*, 283(9), pp.1748–1766.

Gozal, E.A. et al., 2014. Anatomical and functional evidence for trace amines as unique modulators of locomotor function in the mammalian spinal cord. *Frontiers in Neural Circuits*, 8(November), pp.1–20.

Grandy, D.K., 2007. Trace Amine-Associated Receptor 1 – Family Archetype or Iconoclast? *Pharmacology and Therapeutics*, 116(3), pp.355–390.

Harmeier, A. et al., 2015. Trace amine-associated receptor 1 activation silences GSK3ß signaling of TAAR1 and D2R heteromers. *European Neuropsychopharmacology*, 25(11), pp.2049–2061.

Horowitz, L.F. et al., 2014. Olfactory Receptor Patterning in a Higher Primate. *Journal of Neuroscience*, 34(37), pp.12241–12252.

Hussain, A. et al., 2013. High-affinity olfactory receptor for the death-associated odor cadaverine. *Proceedings of the National Academy of Sciences*, 110(48), pp.19579–19584.

Hussain, A., Saraiva, L.R. & Korsching, S.I., 2009. Positive Darwinian selection and the birth of an olfactory receptor clade in teleosts. *Proceedings of the National Academy of Sciences*, 106(11), pp.4313–4318.

Ito, J. et al., 2009. Anatomical and histological profiling of orphan G-protein-coupled receptor expression in gastrointestinal tract of C57BL/6J mice. *Cell and Tissue Research*, 338(2), pp.257–269.

Izquierdo, C. et al., 2018. Identifying human diamine sensors for death related putrescine and cadaverine molecules. *PLoS Computational Biology*, 14(1), pp.1–20.

Janssen, S.F. et al., 2013. Gene Expression and Functional Annotation of the Human and Mouse Choroid Plexus Epithelium. *PLoS ONE*, 8(12), p.e83345.

Johanson, C. et al., 2011. Traumatic brain injury and recovery mechanisms: Peptide modulation of periventricular neurogenic regions by the choroid plexus-CSF nexus. *Journal of Neural Transmission*, 118(1), pp.115–133.

Kang, B. et al., 2018. Characterization of goose SPMS: Molecular characterization and expression profiling of SPMS in the goose ovary. *Reproductive Biology*, 18(1), pp.60–65.

Kang, N. & Koo, J., 2012. Olfactory receptors in non-chemosensory tissues. *BMB Reports*, 45(11), pp.612–622.

Kepp, K.P., 2016. Alzheimer's disease due to loss of function: A new synthesis of the available data. *Progress in Neurobiology*, 143, pp.36–60.

Khan, M.Z. & Nawaz, W., 2016. The emerging roles of human trace amines and human trace amine-associated receptors (hTAARs) in central nervous system. *Biomedicine and Pharmacotherapy*, 83(24), pp.439–449.

Korhonen, V.P. et al., 2001. Spermine deficiency resulting from targeted disruption of the spermine synthase gene in embryonic stem cells leads to enhanced sensitivity to antiproliferative drugs. *Molecular pharmacology*, 59(2), pp.231–238.

Kratzer, I. et al., 2013. Developmental changes in the transcriptome of the rat choroid plexus in relation to neuroprotection. *Fluids and Barriers of the CNS*, 10(1), pp.1–19.

Kubo, H. et al., 2015. Unraveling the Rat Intestine, Spleen and Liver Genome-Wide Transcriptome after the Oral Administration of Lavender Oil by a Two-Color Dye-Swap DNA Microarray Approach. *Plos One*, 10(7), p.e0129951.

Lehtinen, M.K. et al., 2013. The Choroid Plexus and Cerebrospinal Fluid: Emerging Roles in Development, Disease, and Therapy. *Journal of Neuroscience*, 33(45), pp.17553–17559.

Li, Q. et al., 2015. Non-classical amine recognition evolved in a large clade of olfactory receptors. *eLife*, 4(OCTOBER2015), pp.1–17.

Liberles, S.D., 2015. Trace amine-associated receptors: Ligands, neural circuits, and behaviors. *Current Opinion in Neurobiology*, 34, pp.1–7.

Liberles, S.D. & Buck, L.B., 2006. A second class of chemosensory receptors in the olfactory epithelium. *Nature*, 442(7103), pp.645–650.

Lindemann, L. et al., 2005. Trace amine-associated receptors form structurally and functionally distinct subfamilies of novel G protein-coupled receptors. *Genomics*, 85(3), pp.372–385.

Lindemann, L. & Hoener, M.C., 2005. A renaissance in trace amines inspired by a novel GPCR family. *Trends in Pharmacological Sciences*, 26(5), pp.274–281.

Liu, X. et al., 2015. Expression of bitter taste receptor Tas2r105 in mouse kidney. *Biochemical and Biophysical Research Communications*, 458(4), pp.733–738.

Lun, M.P., Monuki, E.S. & Lehtinen, M.K., 2015. Development and functions of the choroid plexus–cerebrospinal fluid system. *Nature Reviews Neuroscience*, 16(8), pp.445–457.

Malki, A. et al., 2015. Class I odorant receptors, TAS1R and TAS2R taste receptors, are markers for subpopulations of circulating leukocytes. *Journal of Leukocyte Biology*, 97(3), pp.533–545.

Marques, F. et al., 2013. Blood-brain-barriers in aging and in Alzheimer's disease. *Molecular Neurodegeneration*, 8(1), p.1.

Marques, F. et al., 2017. Neurobiology of Disease The choroid plexus in health and in disease : dialogues into and out of the brain. *Neurobiology of Disease*, 107, pp.32–40.

Mietz JL, K.E., 1978. Polyamine and histamine content of rockfish, salmon, lobster, and shrimp as an indicator of decomposition. *Journal of the Association of Official Analytical Chemists*, 61(1), pp.139–145.

Minois, N., Carmona-Gutierrez, D. & Madeo, F., 2011. Polyamines in aging and disease. *Aging (Albany NY)*, 3(8), pp.716–732.

Mitchell, S.C. & Smith, R.L., 2001. Trimethylaminuria: The fish malodor syndrome. *Drug Metabolism and Disposition*, 29(4 II), pp.517–521.

Mounce, B.C. et al., 2017. Polyamines and Their Role in Virus Infection. *Microbiology and Molecular Biology Reviews*, 81(4), pp.1–12.

Mühlhaus, J. et al., 2014. Analysis of human TAAR8 and murine taar8b mediated signaling pathways and expression profile. *International Journal of Molecular Sciences*, 15(11), pp.20638–20655.

Nei, M., Niimura, Y. & Nozawa, M., 2008. The evolution of animal chemosensory receptor gene repertoires: Roles of chance and necessity. *Nature Reviews Genetics*, 9(12), pp.951–963.

Nelson, D.A. et al., 2007. Expression of neuronal trace amine-associated receptor (Taar) mRNAs in leukocytes. *Journal Neuroimmunology*, 192(1–2), pp.21–30.

Olson, Maynard V.; Varki, A., 2003. Sequencing the chimpanzee genome: insights into human evolution and disease. *Nature Reviews Genetics*, 4(1), pp.20–28.

Pacifico, R. et al., 2012. An olfactory subsystem that mediates high-sensitivity detection of volatile amines. *Cell Reports*, 2(1), pp.76–88.

Paik, M.J. et al., 2010. Polyamine patterns in the cerebrospinal fluid of patients with Parkinson's disease and multiple system atrophy. *Clinica Chimica Acta*, 411(19–20), pp.1532–1535.

Pegg, A.E., 2016. Functions of polyamines in mammals. *Journal of Biological Chemistry*, 291(29), pp.14904–14912.

Pegg, A.E., 2013. Spermidine / spermine- N 1 -acetyltransferase : a key metabolic regulator. *American Journal of Physiology-Endocrinology and Metabolism*, 294(6), pp.995–1010.

Pei, Y., Asif-Malik, A. & Canales, J.J., 2016. Trace Amines and the Trace Amine-Associated Receptor 1: Pharmacology, Neurochemistry, and Clinical Implications. *Frontiers in Neuroscience*, 10, p.148.

Perez-Leal, O. & Merali, S., 2012. Regulation of polyamine metabolism by translational control. *Amino Acids*, 42(2–3), pp.611–617.

Praetorius, J. & Damkier, H.H., 2017. Transport across the choroid plexus epithelium. *American Journal of Physiology - Cell Physiology*, 312(6), pp.C673–C686.

Qian Li, et al., 2013. Synchronous evolution of an odor biosynthesis pathway and behavioral response. *Current Biology*, 23(1), pp.11–20.

Quintela, T. et al., 2013. Analysis of the Effects of Sex Hormone Background on the Rat Choroid Plexus Transcriptome by cDNA Microarrays. *PLoS ONE*, 8(4).

Rajeeve, V. et al., 2013. Polyamine production is downstream and upstream of oncogenic PI3K signalling and contributes to tumour cell growth. *The Biochemical Journal*, 450(3), pp.619–628.

Ramani, D., De Bandt, J.P. & Cynober, L., 2014. Aliphatic polyamines in physiology and diseases. *Clinical Nutrition*, 33(1), pp.14–22.

Regard, J.B., Sato, I.T. & Coughlin, S.R., 2008. Anatomical Profiling of G Protein-Coupled Receptor Expression. *Cell*, 135(3), pp.561–571.

Revel, F.G. et al., 2011. TAAR1 activation modulates monoaminergic neurotransmission, preventing hyperdopaminergic and hypoglutamatergic activity. *Proceedings of the National Academy of Sciences*, 108(20), pp.8485–8490.

Santos, C.R.A. et al., 2017. The choroid plexus as a sex hormone target: Functional implications. *Frontiers in Neuroendocrinology*, 44, pp.103–121.

Saunders, N.R. et al., 2013. Molecular Aspects of Medicine Transporters of the blood – brain and blood – CSF interfaces in development and in the adult. *Molecular Aspects of Medicine*, 34(2–3), pp.742–752.

Schipper, R.G. et al., 2004. Intracellular localization of ornithine decarboxylase and its regulatory protein, antizyme-1. *Journal of Histochemistry and Cytochemistry*, 52(10), pp.1259–1266.

Schipper, R.G. & Verhofstad, A.A.J., 2002. Distribution patterns of ornithine decarboxylase in cells and tissues: Facts, problems, and postulates. *Journal of Histochemistry and Cytochemistry*, 50(9), pp.1143–1160.

Schmidt-Glenewinkel, T., Nomura, Y. & Giacobini, E., 1977. The conversion of lysine into piperidine, cadaverine, and pipecolic acid in the brain and other organs of the mouse. *Neurochemical Research*, 2(6), pp.619–637.

Simmler, L.D. et al., 2016. In Vitro Characterization of Psychoactive Substances at Rat, Mouse, and Human Trace Amine-Associated Receptor 1 s. *THE JOURNAL OF PHARMACOLOGY AND EXPERIMENTAL THERAPEUTICS*, 357, pp.134–144.

Singh, N. et al., 2011. Functional bitter taste receptors are expressed in brain cells. *Biochemical and Biophysical Research Communications*, 406(1), pp.146–151.

Sotnikova, T.D. et al., 2010. The dopamine metabolite 3-methoxytyramine is a neuromodulator. *PLoS ONE*, 5(10).

Stäubert, C. et al., 2010. Structural and functional evolution of the trace amine-associated receptors TAAR3, TAAR4 and TAAR5 in primates. *PLoS ONE*, 5(6).

Stepita-Klauco, M. & Dolezalova, H., 1974. Cadaverine in the brain of axenic mice. *Nature*, 252(5479), pp.158–159.

Strazielle, N., Khuth, S.T. & Ghersi-Egea, J.F., 2004. Detoxification systems, passive and specific transport for drugs at the blood-CSF barrier in normal and pathological situations. *Advanced Drug Delivery Reviews*, 56(12), pp.1717–1740.

Tabor, C.W. & Tabor, H., 1985. Polyamines in microorganisms. *Microbiological Reviews*, 49(1), pp.81–99.

Tan, E.S. et al., 2009. The molecular basis of species-specific ligand activation of trace amine-associated receptor 1 (TAAR 1). *ACS Chemical Biology*, 4(3), pp.209–220.

Tian, H. et al., 2006. Gene expression of ornithine decarboxylase in lung cancers and its clinical significance. *Acta Biochimica et Biophysica Sinica*, 38(9), pp.639–645.

Tietz, S. & Engelhardt, B., 2015. Brain barriers: Crosstalk between complex tight junctions and adherens junctions. *Journal of Cell Biology*, 209(4), pp.493–506.

Tizzano, M. et al., 2011. Expression of taste receptors in Solitary Chemosensory Cells of rodent airways. *BMC Pulmonary Medicine*, 11(1), p.3.

Tomar, P.C., Lakra, N. & Mishra, S.N., 2013. Cadaverine: A lysine catabolite involved in plant growth and development. *Plant Signaling and Behavior*, 8(10), pp.1–15.

Tomás, J. et al., 2016. "Tasting" the cerebrospinal fluid: Another function of the choroid plexus? *Neuroscience*, 320, pp.160–171.

Vanti, W.B. et al., 2003. Discovery of a null mutation in a human trace amine receptor gene. *Genomics*, 82(5), pp.531–536.

Vattai, A. et al., 2017. Increased trace amine-associated receptor 1 (TAAR1) expression is associated with a positive survival rate in patients with breast cancer. *Journal of Cancer Research and Clinical Oncology*, 143(9), pp.1637–1647.

Wallrabenstein, I. et al., 2013. Human Trace Amine-Associated Receptor TAAR5 Can Be Activated by Trimethylamine. *PLoS ONE*, 8(2).

Wang, J.-Y., 2005. Polyamines regulate expression of E-cadherin and play an important role in control of intestinal epithelial barrier function. *Inflammopharmacology*, 13(1–3), pp.91–101.

Wölfle, U. et al., 2015. Expression and functional activity of the bitter taste receptors TAS2R1 and TAS2R38 in human keratinocytes. *Skin Pharmacology and Physiology*, 28(3), pp.137–46.

Xu, J. et al., 2013. Functional characterization of bitter-taste receptors expressed in mammalian testis. *Molecular Human Reproduction*, 19(1), pp.17–28.

Xueying Ren, Ligang Zhou, Rose Terwilliger, S.S.N. and I.E. de A., 2009. Sweet taste signaling functions as a hypothalamic glucose sensor. *Frontiers in Integrative Neuroscience*, 3(12).

Yatin, M., 2002. Polyamines in living organisms. *Journal of Cell and Molecular Biology*, 1(August), pp.57–67.

Yatin, S.M. et al., 1999. Alzheimer's amyloid ß-peptide associated free radicals increase rat embryonic neuronal polyamine uptake and ornithine decarboxylase activity: Protective effect of vitamin E. *Neuroscience Letters*, 263(1), pp.17–20.

Yoshihara, Y., 2008. Molecular Genetic Dissection of the Zebrafish Olfactory System. *Results and Problems in Cell Differentiation. Author Manuscript*, pp.97–120.

Zucchi, R. et al., 2006. Trace amine-associated receptors and their ligands. *British Journal of Pharmacology*, 149(8), pp.967–978.